Overview of Dynamic Test Techniques for Flight Dynamics Research at NASA LaRC (Invited)

D. Bruce Owens[*], Jay M. Brandon[†], Mark A. Croom[‡], C. Michael Fremaux[§], Eugene H. Heim[**], and Dan D. Vicroy[†]
NASA Langley Research Center, Hampton, VA, 23681

An overview of dynamic test techniques used at NASA Langley Research Center on scale models to obtain a comprehensive flight dynamics characterization of aerospace vehicles is presented. Dynamic test techniques have been used at Langley Research Center since the 1920s. This paper will provide a partial overview of the current techniques available at Langley Research Center. The paper will discuss the dynamic scaling necessary to address the often hard-to-achieve similitude requirements for these techniques. Dynamic test techniques are categorized as captive, wind tunnel single degree-of-freedom and free-flying, and outside free-flying. The test facilities, technique specifications, data reduction, issues and future work are presented for each technique. The battery of tests conducted using the Blended Wing Body aircraft serves to illustrate how the techniques, when used together, are capable of characterizing the flight dynamics of a vehicle over a large range of critical flight conditions.

Nomenclature

b	=	wing span
$\bar{c}$	=	mean aerodynamic chord
C_L	=	lift coefficient
C_l	=	rolling moment coefficient
C_m	=	pitching moment coefficient
C_n	=	yawing moment coefficient
f	=	frequency, Hz
I_{xx}, I_{yy},I_{zz}	=	moment of inertia about the x-axis, y-axis, z-axis, respectively
K	=	a constant
k	=	Strouhal number (reduced frequency), $\omega l/V$
l	=	reference length
M	=	Mach number
$\hat{p},\hat{q},\hat{r}$	=	non-dimensional roll rate, $pb/2V_\infty$; pitch rate, $q\bar{c}/2V_\infty$; yaw rate, $rb/2V_\infty$; respectively
S	=	reference area
V_∞	=	freestream velocity
α	=	angle of attack
β	=	angle of sideslip
σ	=	FS density / MS density
ν	=	kinematic viscosity
ω	=	oscillatory frequency ($2\pi f$), rad/sec
ρ	=	density
12-ft LST	=	12-Foot Low-Speed Tunnel

[*] Aerospace Engineer, Flight Dynamics Branch, M/S 308, Associate Fellow.
[†] Senior Research Engineer, Flight Dynamics Branch, M/S 308, Associate Fellow.
[‡] Senior Research Engineer, Flight Dynamics Branch, M/S 308
[§] Senior Research Engineer, Flight Dynamics Branch, M/S 308, Senior Member
[**] Aerospace Engineer, Flight Dynamics Branch, M/S 308

16-ft TT = 16-Foot Transonic Tunnel
FOM = Figure-of-merit
FS = Full Scale
FTR = Free-to-Roll
LaRC = Langley Research Center
MS = Model scale
N = Scale factor
NTF = National Transonic Facility
R/C = radio-controlled
TDT = Transonic Dynamics Tunnel
UAV = Unmanned aerial vehicle
UPWT = Unitary Plan Wind Tunnel
VST = 20-Foot Vertical Spin Tunnel

I. Introduction

Dynamic test techniques are used at NASA Langley Research Center (LaRC) to conduct research into the flight dynamics of aerospace vehicles. The test techniques are used for dynamic stability measurements, simulation verification, control law design, aerodynamic modeling, spin/tumble prediction, spin/tumble recovery systems, and flying qualities assessments. References 1-4 are a few of the many discussions of dynamic test techniques. Dynamic test techniques aimed at aeroelastic studies are not included in this paper. The categories of dynamic test techniques are captive, wind-tunnel single degree-of-freedom (1-DOF), wind-tunnel free-flying and atmospheric free-flying vehicles. Forced oscillation and rotary balance make up the captive category. These techniques are used to measure the damping and rotary derivatives. The measurements from the forced oscillation and rotary techniques are used along with those from the static tests to develop the math model representation of the aircraft aerodynamics (i.e. the aero-model). The wind-tunnel 1-DOF methods include free-to-roll and free-to-pitch. These techniques are used as intermediate steps to free-flying tests to assess unsteady aerodynamic effects on the motion of the model. These techniques allow rapid assessment of unsteady aerodynamics without the complexity of a free-flying test. Tests using 1-DOF techniques are typically a part of a static force test so the models may not be dynamically scaled. The wind tunnel free-flying methods are free-flight, free-spin, and free-fall. These models are normally dynamically scaled. The free-spin and free-fall techniques are almost exclusively used to study post-stall, equilibrium spin and tumble modes. Also, these techniques can be used to design the spin/tumble recovery systems. The models are typically outfitted with remote actuation of the control surfaces and recovery systems. The models used in the free-flight technique are instrumented to measure all of the aircraft states and air data. Also, they are equipped with a flight control computer so control and/or stability augmentation systems can be implemented. The models are flown with small perturbations about a 1-g, level flight condition. The free-flight technique investigates flying qualities (e.g. departure resistance) and control law effects up to a maximum trim angle of attack or until loss of control occurs. The outside free-flying techniques are drop model and unmanned aerial vehicles (UAV). Both techniques are remotely piloted. The distinct difference between the two is that

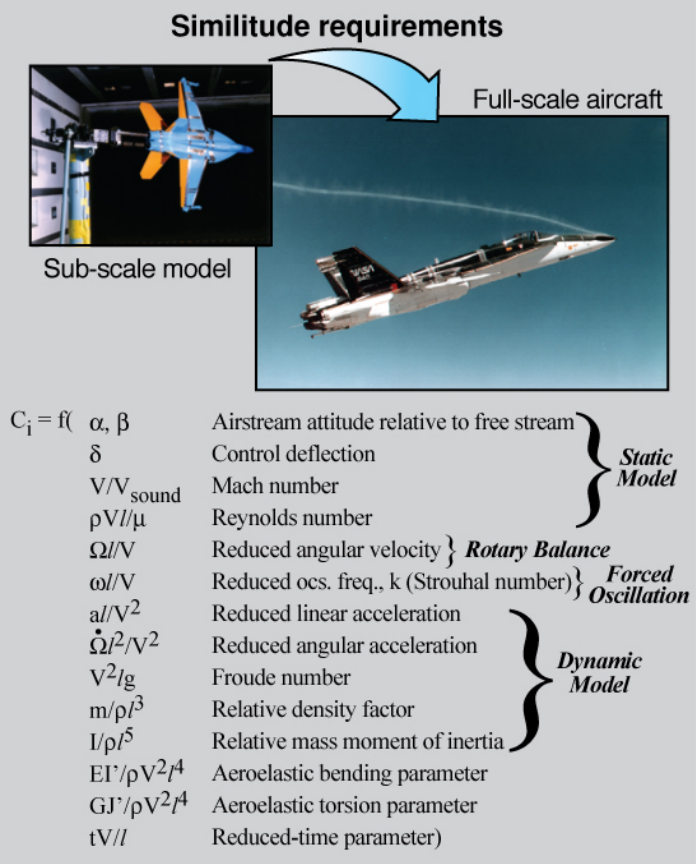

Fig. 1 Similitude requirements

the drop model is typically released at altitude from a helicopter. In this paper they will be generically referred to as remotely piloted vehicles (RPV). Like the wind-tunnel free-flight models the outside free-flying models are dynamically scaled and extensively outfitted with high fidelity instruments to measure aircraft states, air data, and flight systems health. The RPV technique is used to bridge the angle of attack range between the free-flight technique and the free-spin/free-fall techniques. By adhering to the appropriate scaling rules, these model techniques enable accurate predictions of flight dynamics across a wide range of flight phenomena that are difficult if not impossible to ascertain in any other way. Therefore, an aircraft program can use this battery of dynamic test techniques for a comprehensive assessment of the aircraft flying qualities.

Dynamic test techniques at LaRC are conducted in the 12-Foot Low-Speed Tunnel, 20-Foot Vertical Spin Tunnel, 14 X 22-Foot Subsonic Tunnel, National Transonic Facility, Transonic Dynamics Tunnel, and Unitary Plan Wind Tunnel. Although, the Langley Full-Scale Tunnel (formally, the NASA LaRC 30 X 60-Foot Tunnel) is now operated by Old Dominion University this paper reports on a free-flight test conducted in this tunnel. The outside test techniques are conducted at local NASA/FAA approved airfields and at NASA Wallops Flight Facility.

Table 1 Dynamic scaling parameters for Froude scaling.

Parameter	Scale Factor
Linear dimension	N
Relative density ($m/\rho l^3$)	1
Froude number (V^2/lg)	1
Weight, mass	$N^3\sigma^{-1}$
Moment of inertia	$N^5\sigma^{-1}$
Linear velocity	$N^{1/2}$
Linear acceleration	1
Angular velocity	$N^{-1/2}$
Angular acceleration	N^{-1}
Time	$N^{1/2}$
Reynolds number (Vl/ν)	$N^{3/2}\nu/\nu_o$
Dynamic pressure	$N\sigma^{-1}$

Relative to static testing model size, weight, and inertia have significant importance in the dynamic test techniques. This importance is caused by dynamic scaling and/or hardware limitations of the dynamic test rig. Also, most of the test techniques require more complex and expensive hardware than static testing. In the case of the captive techniques the apparatus normally takes up more space behind the model causing support interference effects to be more of a concern than for static testing. In the case of the non-captive techniques rig vibrations, friction, and control surface position repeatability must be addressed.

The discussion of dynamic test techniques will begin with dynamic scaling. A good understanding of the dynamic scaling issues is important in applying data obtained from these techniques. Then the captive techniques will be discussed followed by the 1-DOF techniques. Next, the wind-tunnel free-flying methods will be presented finishing with the outside free-flying techniques.

II. Dynamic Scaling

Full-scale predictions using sub-scale models rely on satisfying a set of similitude requirements. A dimensional analysis of the pertinent parameters for forces and moments was presented in Ref. 5 using the Lord Rayleigh method[6] which results in fourteen dimensionless parameters that represent the requirements for static and dynamic similitude between model and full-scale flight. A summary of these similitude requirements is shown in Fig. 1. As can be seen, accurate predictions of full-scale characteristics require correlation of many, sometimes conflicting, similitude parameters. Although similitude scaling is very important across a range of applications, including aeroelastic modeling, thrust modeling, boundary layer effects, jet interactions, etc., the following will focus on considerations for rigid body dynamic test considerations. A progressive development of the dynamic similitude requirements evolving through geometric, kinematic, and kinetic influences as well as a flight-dynamics specific example of the Rayleigh method are given in Ref. 7.

Various types of wind tunnels and test techniques have been developed largely to address the many similitude requirements. Traditional wind tunnel testing has tried to take into account all of the static model considerations, and also the angular velocity scaling. The

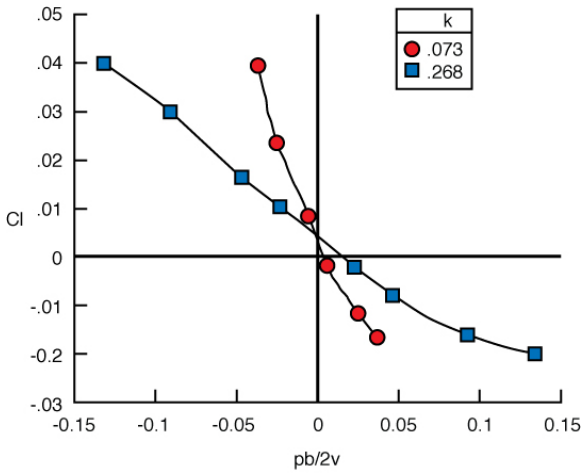

Fig. 2 Effect of Strouhal number (F-16XL, $\alpha = 30°$).

frequency-dependence in the data denoted by the Strouhal number (k, or reduced frequency) was documented in the 1950's, however this effect typically is not addressed in current testing or simulation modeling. The only test method currently in use to obtain k effects is the forced oscillation test; however this data typically is modeled as a linear derivative in non-dimensional rate for only one k value which is usually picked based on estimates of Dutch-roll frequency or short period frequency. Although this method worked well for airplanes in the past, the new realities of operating in highly non-linear flow regimes may have invalidated some of the assumptions and simplifications used previously. The selection of test techniques and conditions need to be made to ensure that the subscale test results will apply correctly to the desired full-scale vehicle.

When predicting static characteristics, for example, flow angles and control surface deflections need to be identical between sub-scale and flight. Mach number and Reynolds numbers also need to be maintained constant between model and flight for the data to be valid as tested. When the airplane is undergoing rotational motions, reduced angular velocity and Strouhal number (frequency content) need to match between model and flight according to the nondimensional analysis results. The frequency content of the motion is one of the scaling parameters that is frequently omitted. In aerodynamic regions with linear responses, neglecting those effects may produce satisfactory results, but when unsteady, nonlinear flow conditions are dominant, the Strouhal number (and probably other time-history effects that are not currently described) can become very important. This effect of Strouhal number is demonstrated in Fig. 2. The figure shows the effect of Strouhal number on rolling moment for a cranked delta wing configuration at $\alpha = 30°$ during a forced oscillation test. The combination of roll rates and oscillation frequencies were arrived at by varying the amplitude of the oscillations, and data were obtained at the midpoint of each cycle – where rate was a maximum and angular acceleration was close to zero. As can be seen the Strouhal effect is significant and therefore should be addressed properly when implementing the simulation aerodynamic model.

Finally, for unconstrained model testing, in order to achieve the same (scaleable) flight dynamics, the model needs to be dynamically scaled by matching of the dynamic parameters (Froude number, relative density factor, relative mass moment of inertia) as shown in Fig. 1.

Correlation of dynamic free-flying test results from scaled model tests to full-scale results of an airplane rely on proper scaling. This means that all of the interactions that are important to result in a full-scale airplane response must be the same for the sub-scale test. Unfortunately, it is rarely possible to accurately scale all of the similitude parameters at the same time. This results in a need to design the test to answer specific questions and focus on scaling the most important parameters to provide the needed results. Several of the listed nondimensional parameters apply to any test – static or dynamic - and the usual requirements of Reynolds number, Mach number, etc. are listed. Some of the more important parameters unique to dynamic testing will be discussed.

Reduced angular velocity is a measure of the angular rate of the airplane. This is the parameter to apply for steady rates, such as those obtained during a steady turn or pull-up. The nondimensional parameter ($\Omega l/V$) represents the induced flow angle at the nondimensional length, l. For instance, for roll, $l = b/2$, and $pb/2V$ gives the induced angle of attack at the wing tip due to the rolling motion. Matching of the reduced angular velocities insures that the distributions of flow angles across the test model are the same as the flight condition.

Reduced oscillatory frequency (Strouhal number) appears very similar to the reduced angular velocity parameter; however Strouhal number is a parameter to account for unsteady aerodynamic effects caused by oscillations of the airplane. Because of unsteady effects, changes in oscillatory frequencies can result in large variation of aerodynamic forces and moments at a given angular rate (Fig. 2).

Froude number was originally developed to provide relationships between forces on a ship hull and the shape of the wave produced. Froude number is used to maintain the ratio of inertia and gravitational effects between a test model and a full-scale vehicle. This is important to insure that the model is maneuvering at the same angle of attack, for example, that the full-scale vehicle would be at for similar flight conditions.

Two primary scaling philosophies are employed when setting up a dynamic sub-scale test. The first option is to scale the test based on Froude number. Matching Froude number will ensure similitude between the model and vehicle angles (attitudes, angle of attack, sideslip, etc), and that the motion dynamics will be properly correlated between the model and full-scale vehicle. The second philosophy is Mach scaling. This method is used when it is expected that compressibility effects will be significant. With Mach scaling (unless Froude number is

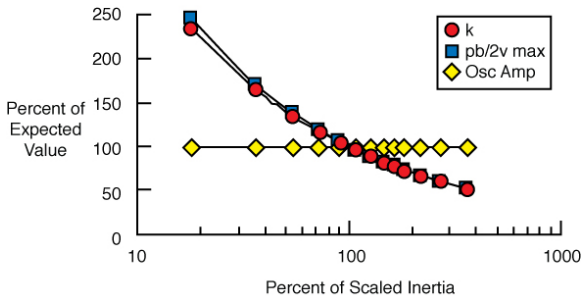

Fig. 3 Typical impact of inertia scaling on roll motions observed for linear damping model

also matched), model and full-scale attitudes will not be matched, so that stability and control effects which are strong nonlinear functions of the vehicle state will not be well simulated in the model tests. For stability and control tests, typically Froude scaling is used. A set of scale factors for providing Froude scaling are shown in table 1.

For a completely free-flying model, construction of the model needs to properly scale the weight, and then the model needs to be tested in a facility where the dynamic pressure is scaled according to table 1. That will ensure that the model is flying at the correct angle of attack. The correct scaling of dynamic responses requires the moments of inertia to be scaled correctly. This is usually a difficult task, since the scaling is a factor of N^5, and results in very difficult model construction – especially as the scale factor decreases. It is important to note that with the Froude scaling, and use of typical wind tunnels and model scales, Reynolds number and Mach number will not be correctly scaled. Often for low Mach number flight, compressibility effects are negligible (for instance if looking at high-α characteristics), and for configurations with sharp leading edges, strakes, etc. where flow separation is fixed, Reynolds number may not be a large factor either. For high-lift configurations such as slotted flaps, leading-edge flaps with gaps, or for relatively blunt surfaces such as thick wings or large smooth forebodies, Reynolds number may have a dominant impact.

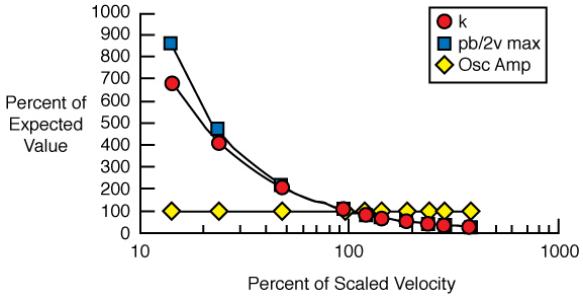

Fig. 4 Typical impact of velocity scaling on roll motions observed for linear damping model.

As previously mentioned a problem for dynamic testing – even more than for captive testing – is difficulty in constructing the models and tests to satisfy the similitude requirements. Therefore, many times, trade-offs must be made. For example for free-flying tests, it has been found that if the inertia scaling is impossible, at least scaling of the inertia ratios is important, so that the initial coupling between the motion axes are correctly represented (i.e. angular accelerations occur at the same relative magnitudes). Even with matching inertia ratios, motion coupling due to rates will not be correctly represented. The problem of getting scalable results with incorrect inertias can be seen by examining the equations of motion. For illustration, the moment equations are written in non-dimensional form:

$$C_l = \frac{I_{xx}}{\frac{1}{8}\rho S b^3}\hat{\dot{p}} + \frac{(I_{zz}-I_{yy})}{\frac{1}{8}\rho S b^2 \bar{c}}\hat{r}\hat{q}\ ;\ C_m = \frac{I_{yy}}{\frac{1}{8}\rho S \bar{c}^3}\hat{\dot{q}} + \frac{(I_{xx}-I_{zz})}{\frac{1}{8}\rho S b^2 \bar{c}}\hat{p}\hat{r}\ ;\ C_n = \frac{I_{zz}}{\frac{1}{8}\rho S b^3}\hat{\dot{r}} + \frac{(I_{yy}-I_{xx})}{\frac{1}{8}\rho S b^2 \bar{c}}\hat{p}\hat{q}$$

It can be seen that for a given rolling moment coefficient (correct geometry scaling), an incorrect I_{xx} (say, $I_{xx\text{-}actual} = I_{xx}*K$) will result in incorrect roll rate acceleration. The initial angular acceleration will be the desired acceleration/K. If each inertia value is scaled such that the inertia ratios are correctly scaled, then the initial non-dimensional angular accelerations will all be similarly reduced by the factor K. The integration of the angular acceleration will produce rates that are also reduced by the factor of the mismatch in inertia values; however the rate coupling term will then be reduced by a factor of $1/K^2$ due to the product of the rates. This will result in slightly incorrect relative magnitudes of the inertial coupling results – in addition to rates and accelerations that are not scaled completely. For small errors in inertias, and for low rates, this may be negligible.

Turning to a more constrained problem – scaling requirements for one-dimensional degree-of-freedom tests such as free-to-roll – allows simple calculations to explore scaling issues. Simplifying the problem to one axis of concern removes issues of coupling effects, and results in the usual static test requirements (Mach,

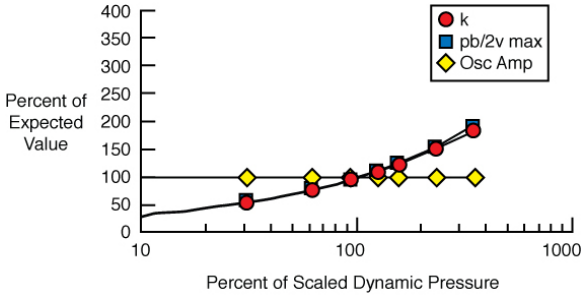

Fig. 5 Typical impact of dynamic pressure scaling on roll motions observed for linear damping model.

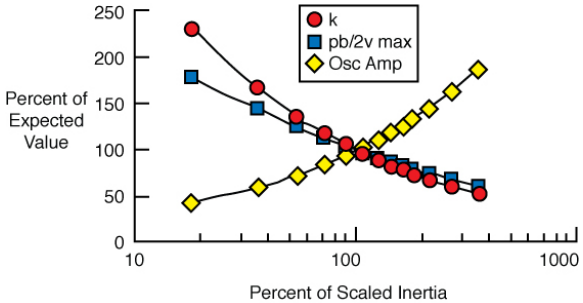

Fig. 6 Typical impact of inertia scaling on roll motions observed for nonlinear damping model.

Reynolds, geometry, α, β, …) and proper scaling of the roll axis inertia and velocity and dynamic pressure. In practice, for transonic tests, models tend to be very dense and the roll inertias tend to be orders of magnitude greater than required for Froude scaling. What impact does the improper scaled inertia have on the expected results? Unfortunately, the impact is very much a function of what the actual aerodynamic physics are on the model. If the aerodynamics are linear – such as C_{l_β} and C_{l_p} linear in sideslip and roll rate, respectively, then the effect of the improperly scaled inertia and tunnel speed are easy to determine. For example, for a model correctly scaled in Mach and density ratio, the effect of inertia scaling errors on maximum reduced roll rate might look like Fig. 3. Figure 3 shows that for inertias less than appropriately scaled values, the observed roll rates will be greater than expected. Conversely, with larger inertias (normally the case for wind tunnel tests), the observed roll rates will be less than expected. Similar plots can be constructed for effects of mismatches in scaled velocity or dynamic pressure, and are shown in Figs. 4 and 5. The analysis shows that if the aerodynamics exhibit linear damping with respect to roll rate, the oscillation amplitude response is not affected by mismatches in scaling parameters of velocity and dynamic pressure, however the roll rate is mispredicted with improper scaling of these parameters.

Unfortunately, critical flight conditions often are in regions of separated flow and therefore may exhibit significant aerodynamic nonlinearities in static and dynamic stability. So, the very parts of the flight envelope that high fidelity aerodynamic math models are needed to prevent departures or other undesirable flight dynamics problems are the same conditions where the most uncertainties occur. Using the same general model as before, but including an effect of roll damping varying with roll rate produces the following results. Figure 6 shows the effect of inertia scaling with the nonlinear rate damping. As can be seen, now all roll parameters vary with the inertia in nonlinear fashions. Of particular note is that now none of the parameters can directly compare with the full-scale case.

A similar result is seen for variations of velocity scaling (Fig. 7) and dynamic pressure scaling (Fig. 8). The results indicate that unless the model structure of the aerodynamics is well known, incorrect dynamic scaling will result in incorrect predictions of motion, which are not readily corrected to full-scale flight values. On the other hand, for a 1-DOF example such as presented here, if the aerodynamic model is well known (for instance at low angles of attack), then the results from an un-scaled test could be related by use of analysis such as presented here.

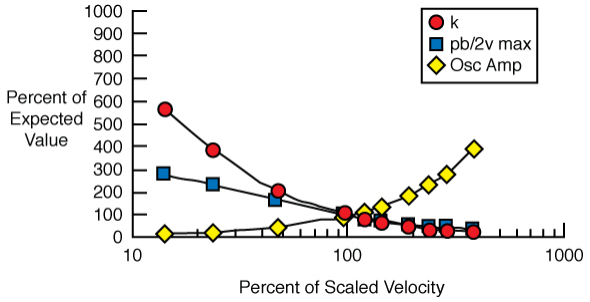

Fig. 7 Typical impact of velocity scaling on roll motions observed for nonlinear damping model.

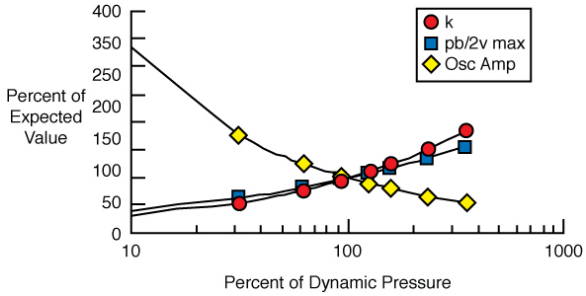

Fig. 8 Typical impact of dynamic pressure scaling on roll motions observed for nonlinear damping model.

III. Forced Oscillation

The forced oscillation tests involve models rigidly mounted on a support system which is then actuated to impart motion to the model while measuring forces and moments acting on the model. Forced oscillation testing covers a broad range of test motions and test rigs across several wind tunnel facilities. Motion shapes can be of many forms. Traditional forced oscillation testing involved the use of sinusoidal motions, but due to nonlinear aerodynamic response with motion parameters, use of alternate motion shapes such as frequency sweeps or Schroeder sweeps have also been used more recently to improve data content and test efficiency.

At NASA LaRC the forced oscillation technique is conducted in the 12-ft LST, 14-by-22-Foot Subsonic Tunnel, VST, TDT, NTF, and the UPWT to cover the speed range of $0 < M < 4.6$. The forced oscillation rigs used in the first three tunnels just listed will be discussed in this paper while the rig used for the remaining tunnels is discussed in Ref. 8.

Forced oscillation tests were conducted for decades in the 30-by-60-Foot Tunnel using a sinusoidal oscillating test rig. When NASA discontinued use of the 30-by-60 Foot Tunnel in 1995, the forced oscillation test rig was modified for use in the 14-by-22-Foot Subsonic Wind Tunnel. Since that time, it has had several upgrades, and is still being used in testing. The forced oscillation rig (shown in Fig. 9 with model mounted for roll, yaw, or pitch oscillation testing) consists of a motor and a gearbox that drive a flywheel. A vertical push rod connects the flywheel to a bellcrank that in turn is attached to a sting. The model is attached to the sting through an internally mounted 6-component strain gauge balance. The motor RPM can be adjusted to control the oscillation frequency (0.1 to 1.0 Hz), and the radial location on the flywheel where the pushrod is mounted can be varied to set the oscillation amplitude (up to 30 degrees).

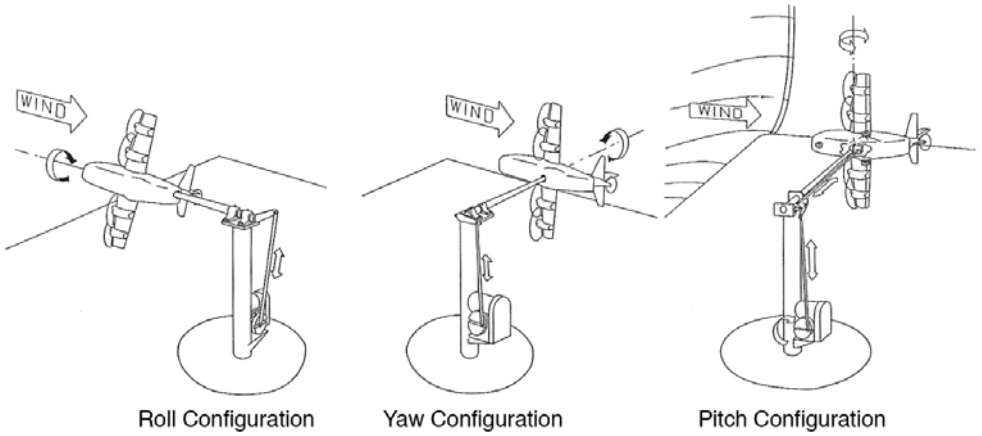

Fig. 9 Current 14-by-22-Foot Subsonic Wind Tunnel forced oscillation capability.

The setup for yaw oscillation is the same as roll, except that the sting is attached through either the top or the bottom of the model. For pitch oscillation, again the model is mounted with the wings in the vertical position, but the pushrod from the flywheel is attached to a different oscillation mechanism that uses a yoke arrangement to connect to the balance, with a pushrod rotating the balance/model about the pivot point on the yoke (Fig. 9). For all setups, with the vertical wing position, α is varied by rotation of the entire support system on a turntable mounted in the tunnel. The location of the forced oscillation rig, and length of sting is designed such that the model reference location remains in the same spot in the tunnel at any α. If data at sideslip is required, then the model must be rotated on the sting – which is a relatively labor intensive operation, and combinations of rotation, and pitch angle are used to obtain β. The kinematic relationships result in varying β with changes of turntable (pitch) angle, so developing a matrix of data at α and β is extremely time consuming and labor intensive.

The 12-ft LST is best used as a concept development environment due to its easy access to the test section, low operating cost, and large range of test capabilities including static & dynamic testing, force & moment measurements, pressure measurements, ease of flow visualization with smoke and laser light sheet, tufts, oils, or other means. The 12-ft LST typically conducts testing at 4 psf dynamic pressure, though it can be operated from about 0.25 to 7 psf. The tunnel currently has two captive dynamic test rigs available for use – the dynamic pitch rig and the roll oscillation system. The dynamic pitch rig is a computer controlled, hydraulically actuated system that is sting-mounted on a C-strut support system (Fig. 10). The mounting arrangement rotates the model about the

moment reference center of the internally mounted balance, over a total angle of attack range of about 85°. The maximum capability of the dynamic test rig is 260 deg/sec pitch rate, and 2290 deg/sec^2 pitch acceleration. The dynamic pitch rig can be set at discrete sideslip angles, and can also test a wide variety of pitching motion shapes. Some of the motion shapes tested include sinusoidal oscillations of various amplitudes and frequencies, ramp motions (constant pitch rate), sum of sinusoidal motions at various frequencies and amplitudes, and Schroeder sweeps. Further description of the dynamic pitch rig may be found in Ref. 9-11.

Data recorded during a test run include pitch angle from a linear variable differential transformer (LVDT), six-component force and moment data from a strain-gauge balance, and freestream dynamic pressure from a wall-mounted pitot-static probe. Data typically are sampled at 100 Hz with an in-line low-pass anti-aliasing filter. All data channels are subsequently digitally filtered and several cycles of testing are ensemble averaged to reduce data scatter.

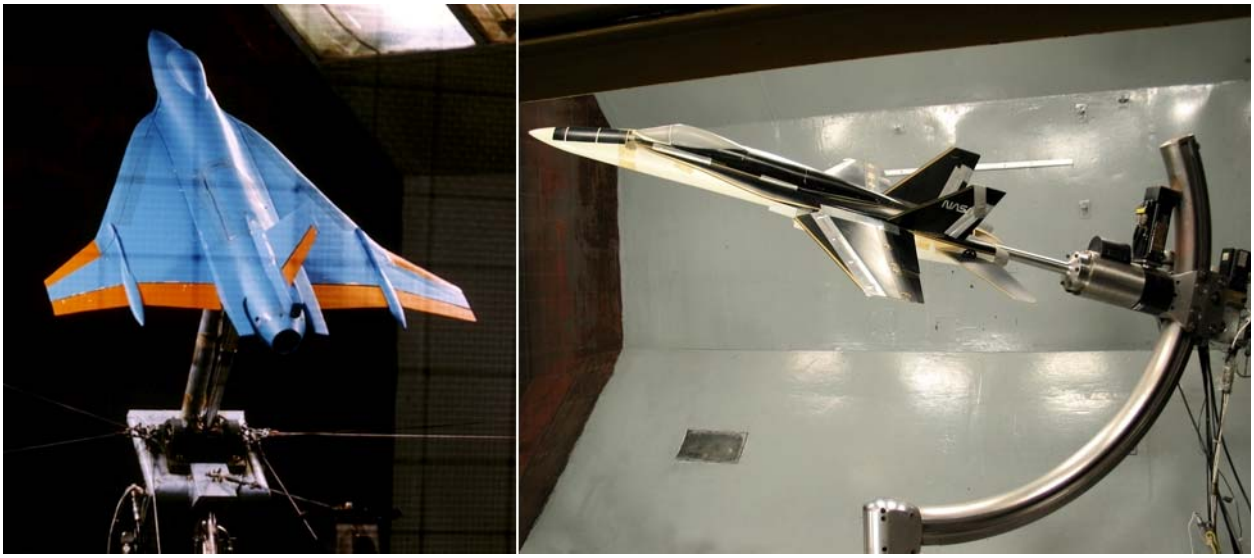

Fig. 10 12-ft LST Dynamic Pitch Motion Test Rig (left) and Roll Oscillation System (right).

A recent addition to testing capabilities in the 12-ft LST is the addition of the Roll Oscillation System (ROS). The ROS consists of a computer controlled electromechanical actuator mounted on the C-strut model support. The ROS allows a model to be sting-mounted through the rear of the model for conventional static and dynamic roll tests. Also, the model can be sting mounted from the top or bottom of the model for dynamic yaw tests. In addition to programmable motion shapes, a key element of the ROS is that it enables independent testing of α and β combinations which were previously very difficult to obtain with the conventional system. For example, when the model is rear mounted (Fig. 10) it can be oscillated with wings nominally level and α obtained with the normal increase of pitch angle on the sting, and β obtained by rotating the C-strut – just as done for normal static testing. Alternately, the model can be tested with the wings positioned vertically, β set by movement of the sting pitch angle, and α set by rotation of the C-strut. This allows for the first time the capability to develop "square" data bases with the dynamic data as function of α and β. It also makes possible the use of the modern design of experiments. The ROS motion capabilities are ±170 deg. in roll with a maximum rate and acceleration of 190 deg/s and 12,750 deg/s^2, respectively. The maximum acceleration during a test of a specific model/balance combination is software limited to not exceed balance limits.

The forced oscillation test technique used for the transonic and supersonic regimes is called the LaRC Dynamic Stability Research System (DSRS). This system uses special oscillating balances and, since it is a mobile unit, is used in the TDT, NTF, and UPWT. This test technique involves oscillating the model in a single degree-of-freedom at the natural frequency of the model/balance system during testing. A brief summary of the technique will be given here but details of the technique are listed in Ref. 8.

Accurate modeling of dynamic derivatives outside the low speed regime has been a long-standing problem throughout the industry. A recent upgrade of the DSRS addresses this issue by enabling the acquisition of dynamic data previously unattainable in transonic and supersonic conditions due to the lack of technology and tool development. These upgrades have involved all new instrumentation, test hardware and software development

utilizing reduction methodologies that can now capture non-linear rate effects in transonic and supersonic conditions. The DSRS has recently demonstrated the ability with a 1/17th-scale Joint Strike Fighter model in the TDT. The test technique successfully confirmed the ability to acquire "specific point" data at varying angular rates in pitch, roll and yaw in both low and high-speed regimes, as well as preserving historical forced oscillation capability. The upgraded system is now capable of developing a database of periodic model behavior at high risk, unsteady aerodynamic conditions. The test method can populate a database with specific angular rate data, hence providing much higher fidelity vehicle simulations in high speeds during design and prior to flight test stages. This type of dynamic data acquisition has previously only existed in the low speed realm and has never been possible before in transonic and supersonic speeds. This technique now eliminates the need to simulate and extrapolate dynamic aerodynamic terms at these high-speed conditions and is an important step forward in the support of experimental databases for computational simulations.

Data reduction for the 14-by-22 Foot Subsonic Tunnel Apparatus

Forced oscillation is a key source of dynamic aerodynamic information for aircraft simulation and modeling particularly for measuring body axis damping derivatives. Traditional forced oscillation tests consist of sinusoidal motions with a single frequency and prescribed amplitude about a fixed body-axis, i.e. pitch, roll or yaw. Typically only frequencies near the Dutch roll natural frequency and short period natural frequency of the aircraft were tested over small amplitudes to estimate damping derivatives[12,13]. These damping derivatives were then assumed to be linear with angular rate. The primary averaged in-phase and out-of-phase (damping) coefficients from forced oscillation about the each body axis are given in table 2. Note the dependence on rates due to the kinematic coupling of oscillation about the body axis.

Table 2 Primary averaged in-phase and out-of-phase body axes moment coefficients

Oscillation axis	In-phase	Out-of-phase (damping)
Pitch	$\overline{C_{m_\alpha}} = C_{m_\alpha} - k^2 C_{l_{\dot{q}}}$	$\overline{C_{m_q}} = C_{m_q} + C_{m_{\dot{\alpha}}}$
Roll	$\overline{C_{l_\beta}} = C_{l_\beta} \sin(\alpha) - k^2 C_{l_{\dot{p}}}$	$\overline{C_{l_p}} = C_{l_p} + C_{l_{\dot{\beta}}} \sin(\alpha)$
Yaw	$\overline{C_{n_\beta}} = C_{n_\beta} \cos(\alpha) + k^2 C_{n_{\dot{r}}}$	$\overline{C_{n_r}} = C_{n_r} - C_{n_{\dot{\beta}}} \cos(\alpha)$

Historically hardware integrators were used to average the in-phase and out-of-phase balance loads with angular position based on the voltage output of the balance and a precision sin-cosine potentiometer which was coupled directly to the flywheel of the 14-by-22-Foot Subsonic Wind Tunnel forced oscillation system (hence these coefficients are often referred to as integrated coefficients). As computer and data acquisition systems advanced the in-phase and out-of-phase coefficients were calculated by a computer after acquiring the balance and precision sin-cosine potentiometer signals. Recent improvements in computer processing and data storage capabilities have allowed analysis of force and moment time histories during the tests thus enabling further data reduction schemes to be explored[14,15].

The current data reduction process for forced oscillation testing is somewhat similar to that of static testing. The first difference arises from a purely operational inconvenience. Static model support systems are typically easily positioned so that balance voltage offsets or zeros can be recorded and later removed from static measurements. The forced oscillation rig however, allows no direct control of the position of the model about the oscillation axis. Oscillations can only be turned on or off so the model must be manually set to a reference position if desired. This process is cumbersome and time-consuming so no electrical zeros are acquired. A consequence of not removing zeros is that tares and runs must be recorded back-to-back with the assumption that the electrical offsets do not change. The tares are oscillated at the same amplitude and frequency as the planned run, however; tares are only recorded at one attitude, typically at zero α, as the gravity vector with respect to the model is assumed not to change as the turntable is positioned. After data is acquired the balance interactions are applied and the voltages converted to engineering units.

Traditionally data is sampled at 200 Hz for 40 sinusoidal periods or 40 cycles. Variable frequencies and amplitudes with a fixed sample rate give rise to variable position samples. Therefore, samples are not recorded at the same cycle position for each cycle. For this reason each cycle must be interpolated from the data acquisition time-stamp time-history. Cycle endpoints are found by interpolating the time where the angular position is zero and

the angular rate is positive. All signals are then interpolated from 0 to 2π over each cycle for *N* number of points (typically 100). Each interpolated point is then averaged across all cycles to produce one ensemble averaged cycle. This averaged cycle then serves as a weight and inertial tare. Wind-on runs are reduced following the same procedure. The tare is then subtracted and the forces and moments converted to coefficients.

The standard sample period of 40 cycles for forced oscillation tests was selected based on comparing the change in the integrated coefficients over a wide range of α's for several models of various configurations. The large cycle count was primarily influenced by regions near and post stall, which require longer sample periods to estimate a "good" mean. Relatively benign regions, such as the linear region of the lift curve, are often over sampled (particularly wind-off tares). A more efficient process of acquiring forced oscillation data has been developed based on monitoring the rate of change of uncertainty of the mean cycle during acquisition (Ref. 16).

Example data set

Each cycle produces a hysteresis loop of the aerodynamic coefficients when plotted verses the angle about the axis-of-oscillation if there is any aerodynamic damping. The hysteresis loops contain information vital to aircraft stability analysis. For example Fig. 11 is a typical rolling moment coefficient hysteresis loop for all 40 continuous cycles and the mean interpolated cycle. The inclination of the loop has a negative slope. This negative slope implies a negative C_{l_β} which is necessary for stability. The arrows on the loop show the direction of the cycle. The breadth of the loop (along the C_l axis) is indicative of the magnitude of C_{l_p}. For roll stability C_{l_p} must also be negative. This requires a counter-clockwise loop direction, which is shown. Any crosses or twists in the loops signify a change of sign of the rate-damping derivative.

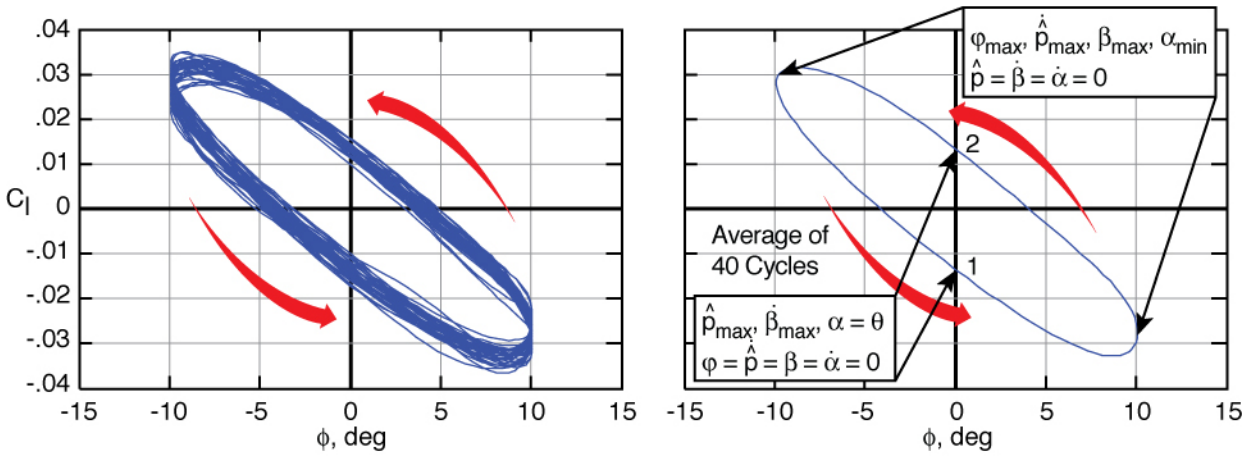

Fig. 11 Time history of rolling moment coefficient verses roll angle for 40 continuous cycles (left) and the average cycle (right)

Forced oscillation tests have documented effects of reduced frequency, $\omega l/V_\infty$, since the 1960's[13], however modeling of those effects has only recently begun to be addressed in current testing and simulation. This effect of reduced frequency may be an indication of time-dependence in the aerodynamic response due to model motion. Figure 12 shows the variation of the out-of-phase and in-phase coefficients with reduced frequency for the F-16XL. Conventional single-frequency forced oscillation testing leads to a very large test matrix. Wide-band frequency inputs such as Schroeder sweeps can be used to collapse test matrices thus saving time and effort. Schroeder chirps are designed such that the power over a frequency range is constant with an amplitude that is limited to a maximum range. The damping and unsteady terms are still combined in the Fourier coefficients as with discrete frequencies. However, wide-band inputs can be used to obtain damping and unsteady terms as a continuous function of frequency (Fig. 13). Future plans include arbitrary motion paths with multi-degree-of-freedom test rigs (Fig. 14).

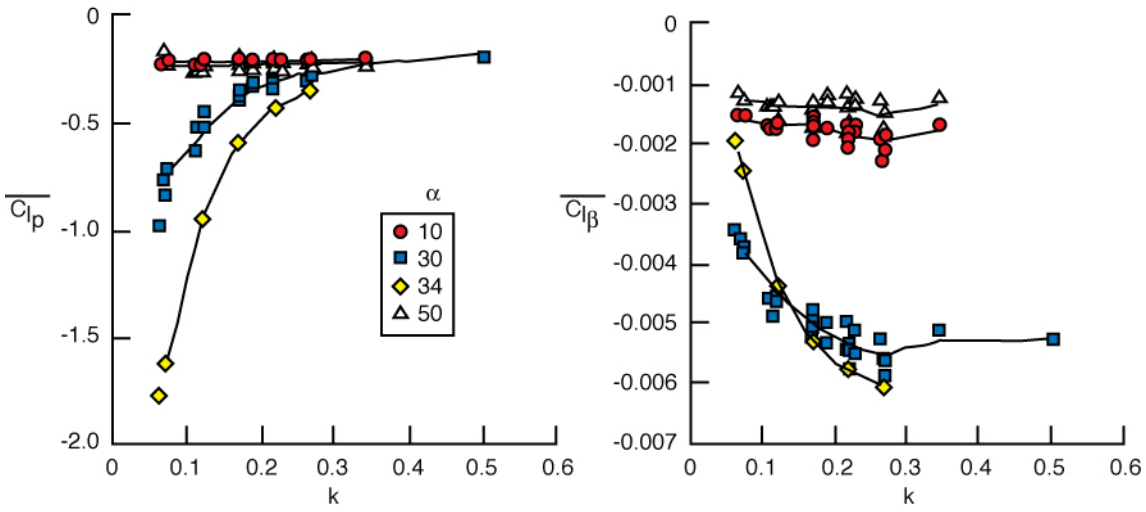

Fig. 12 Variation of out-of-phase and in-phase coefficients with reduced frequency.

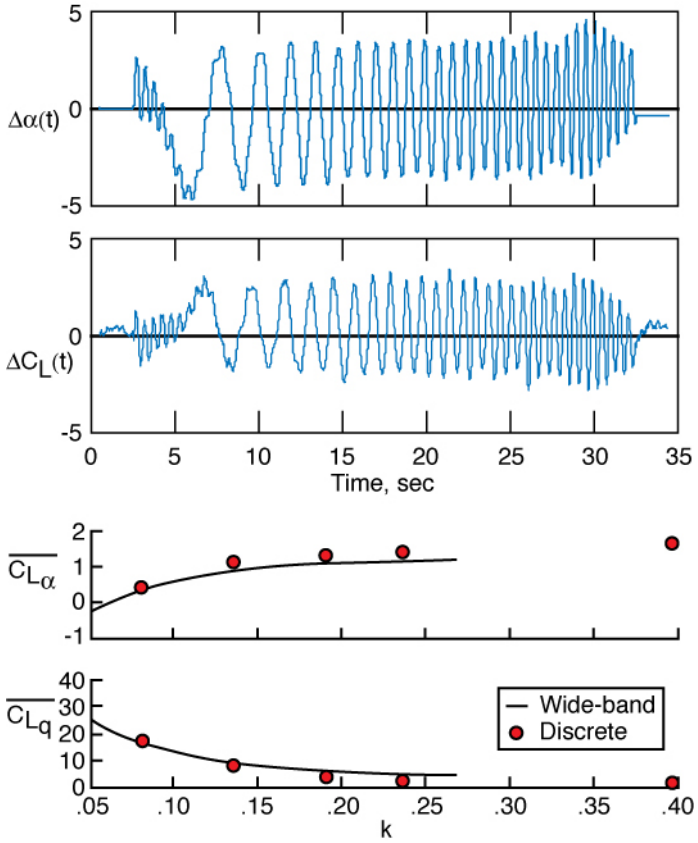

Fig. 13 Schroeder sweep used to acquire wide-bandwidth frequency dependents.

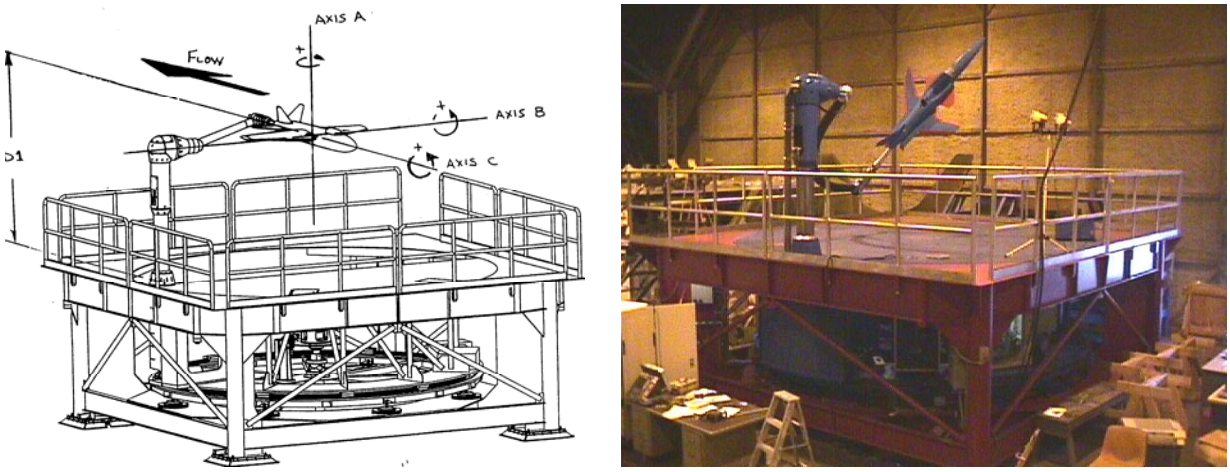

Fig. 14 14-by-22-Foot Subsonic Wind Tunnel multi-axis arbitrary motion forced oscillation cart.

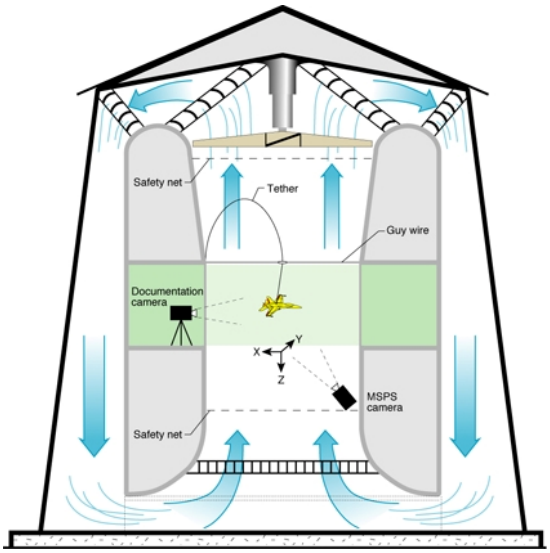

Fig. 15 Typical test setup in for free-flying models in VST.

IV. Rotary Balance and Combined Motion

Tests of captive dynamic models have been conducted since the 1920s and dynamically scaled, free-flying models since the mid-1930s[17], and since the early 1940s in the current VST. The tests in the VST are used to study airplane spin and spin-recovery characteristics, emergency spin recovery parachute requirements, dynamic stability of free-falling bodies (such as non-lifting atmospheric entry vehicles or ordinance packages), and tumble characteristics (i.e., autorotation in pitch) of tailless configurations or various other shapes. A cutaway drawing of the VST (Fig. 15) shows the general layout of the tunnel, where either a captive model or free-flying model can be tested (free-flying model shown). The VST is equipped with two separate data acquisition systems for use with its primary test techniques. For captive model techniques, forces, moments, and surface pressures are measured and recorded and reduced to coefficient form for later analysis. The second system is for tracking the position and attitude of free-flying models, which will be described in a later section.

Captive tests performed in the VST include static force and moment, rotary balance (forces and moments measured under steady rotation about the velocity vector, or "coning"), surface pressures during static and coning tests, and unsteady body-axis forced oscillation. The VST is also well suited to assessing the performance and stability characteristics of small parachutes. Forced oscillation capability is currently in the process of being developed as part of the rotary balance system (to provide so-called "combined motion" or "oscillatory coning") and will be briefly summarized.

Fig. 16 Rotary balance test of 2% BWB in VST.

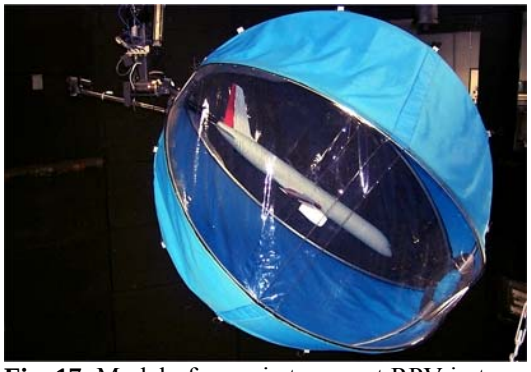

Fig. 17 Model of generic transport RPV in tare bag for rotary balance test in VST.

Rotary balance testing

Rotary balances were first put into operation at NACA Langley in the late 1920s, when the 5-foot vertical tunnel was put into operation[18]. Several new balances have been developed and used over the years, up to the current rig in the VST that became operational in 1992. Data from rotary balance tests are used for analyzing subsonic rate damping characteristics, predicting spins, and for implementation of spin modeling in high-fidelity 6-DOF simulations.

In rotary balance tests, a model is sting-mounted on an arm in the VST test section (Fig. 16) and rotated at up to 68 RPM in either a clockwise or counter-clockwise direction so that data can be obtained for both positive and negative values of non-dimensional spin rate (i.e., velocity-vector roll rate non-dimensionalized by model wing span and test section velocity). The center of rotation is typically the nominal vehicle center of gravity location, but a nonzero "spin radius" (i.e., the distance from the c.g. to the center of rotation) can be accommodated. The rig is capable of setting angles of attack between 0 and 90 degrees, and angles of sideslip from -45 degrees to +45 degrees.

Due to the rotation of the model, the internal strain gage balance senses the sum of the aerodynamic as well as inertial forces and moments acting on a model. Ideally, the model would be rotated in a vacuum at the same attitudes and rates used in the air-on test to obtain the inertial contributions, or "tares". These tares would then be subtracted from the air-on measurements resulting in the "pure" aerodynamic contributions. Since it is not possible to evacuate the test section, a practical solution is to rotate the model while encapsulated in a "tare bag" (Fig. 17) that remains stationary relative to the model while the rig is rotating. Once a steady rotation rate is reached (and after a reasonable settle time) the air in the bag should rotate with the model and thus not provide an aerodynamic contribution. These tares are then subtracted from the air-on forces and moments in order to determine the rotational aerodynamics of the configuration.

An example of data from this type of test (after subtraction of the tares) is presented in Fig. 18. In this plot, body axis yawing moment coefficient is plotted against non-dimensional spin rate for various angles of attack at zero sideslip. Note that quadrants I and III indicate "damping" (moment resisting direction of model rotation), while quadrants II and IV are "propelling" (moment in same direction as model rotating).

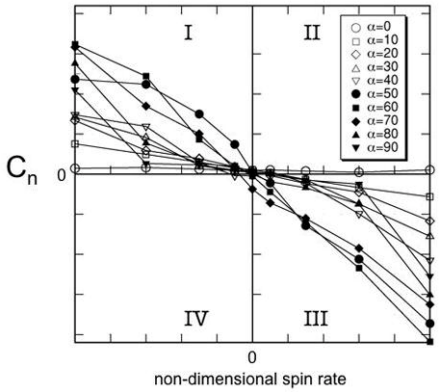

Fig. 18 Typical rotary balance data.

Steady spin prediction using rotary balance data

Rolling moment, yawing moment, and pitching moment coefficient data from rotary balance tests (similar to that shown in Fig. 18) are used as inputs to a three degree-of-freedom (3-DOF) spin prediction program. This custom software was developed for NASA using the algorithms outlined in Refs. 19-21. Briefly, a steady spin can be modeled as a 3-DOF phenomenon by considering three moments and making some simplifying assumptions. The software sequentially sifts through the data sets and determines the combination(s) of angle of attack, sideslip angle, rotation rate, and dynamic pressure, if any, that result in a balance between the measured aerodynamic moments and the full-scale airplane inertial moments. Simple stability criteria are then used to determine whether any of these "crossings" are stable. In this way, different mass loadings, control configurations, etc., can be quickly analyzed for their effect on airplane spin characteristics. Both "pro-spin" and "anti-spin" control deflections are usually considered. The method is capable of predicting steady-state spins only, i.e. real spins always exhibit some degree of oscillation, especially in α and β, but only the mean values of the oscillations are calculated with this method. In some cases, oscillations during the spin of an airplane (or a dynamically scaled model) may be so violent that equilibrium cannot be maintained and the airplane will pitch or roll out of the spin without any recovery-control inputs. Also note that while this method can determine whether or not a given control combination results in a spin, it cannot be used to predict the number of turns needed for recovery. That is, if a spin mode exists for a given combination of control surface deflections, this method cannot be used to determine whether recovery will require 1 turn or several turns. Free-spin tunnel tests and outdoor drop tests using dynamically scaled models are typically used for this purpose. Six degree-of-freedom simulations may also be used once they have been "calibrated" against some form of experimental data.

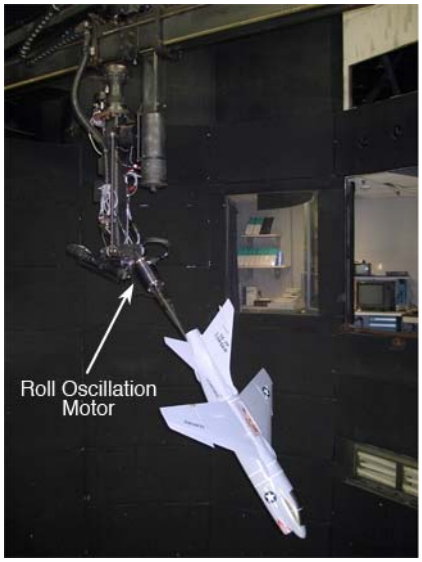

Fig. 19 Modular roll oscillation mechanism installed on VST rotary balance.

Combined motion testing

NASA Langley is in the process of upgrading the VST rotary balance rig to include forced oscillation with the goal of providing so-called "combined motion" or "oscillatory coning" (i.e., simultaneous body-axis oscillation superimposed on steady coning) to provide off-axis dynamic data to aid in simulating complex maneuvers and out-of-control modes such as oscillatory spins. Currently, a small, modular roll oscillation mechanism can be installed

on the rig between the mounting flange and sting flange (see Fig. 19), allowing standard (i.e., without coning motion) forced oscillation tests to be performed in a manner similar to that described in an earlier section. Hardware and rig control system software upgrades are in progress to allow combined motion in both roll and yaw axes. In addition, a preliminary design study is underway for adding pitch oscillation. When completed, the rotary rig will have the capability of performing combined motion tests about any of the three axes, similar to that of the Multi-Axis Test (MAT) rig at Wright-Patterson Air Force Base[22].

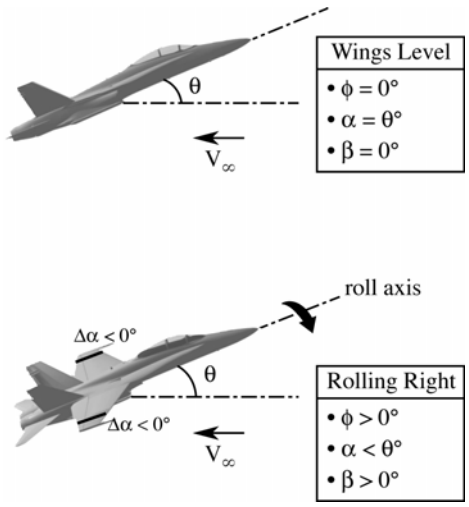

Fig. 20 Kinematic relationships during rolling motion at a fixed pitch and yaw angle.

V. Free-To-Roll

The FTR test technique has been used at LaRC to assess the low-speed, high angle-of-attack characteristics of high-performance aircraft configurations for several decades. These tests have been used to successfully predict and analyze uncommanded rolling motions for generic and scaled models. In general, the FTR test technique allows the model to develop rolling motion that is a response to unsteady, non-linear aerodynamics. Recently, as a part of the Abrupt Wing Stall (AWS) program (Refs. 23-25) an exploratory transonic FTR test was conducted with a 9% pre-production F/A-18E model in the TDT. This highly successful pathfinder test proved the utility of the FTR test technique in evaluating the uncommanded lateral motions of the pre-production F/A-18E. Based on the success of this pathfinder study, an operational test apparatus and technique was developed for the 16-ft TT to permit FTR studies for other military aircraft configurations. The tests were designed to evaluate the FTR test technique as a tool during normal transonic stability and control static force tests. Therefore, the FTR rig was designed with the objectives of using existing transonic wind-tunnel models and allowing rapid transition from the static test technique to the dynamic test technique with the same model in the same tunnel entry[24]. With the closing of the 16-ft TT in September of 2004 the FTR rig was transitioned to the NTF at LaRC. After a successful FTR test of a Joint Strike Fighter model in the 16-ft TT, the Calspan Corporation built a FTR rig based on the 16-ft TT FTR rig for the Calspan 8 Foot Transonic Tunnel (Ref. 26). With the successful implementation of a FTR rig in the Calspan tunnel, Lockheed-Martin currently uses the FTR technique as a normal part of their JSF stability and control tunnel tests.

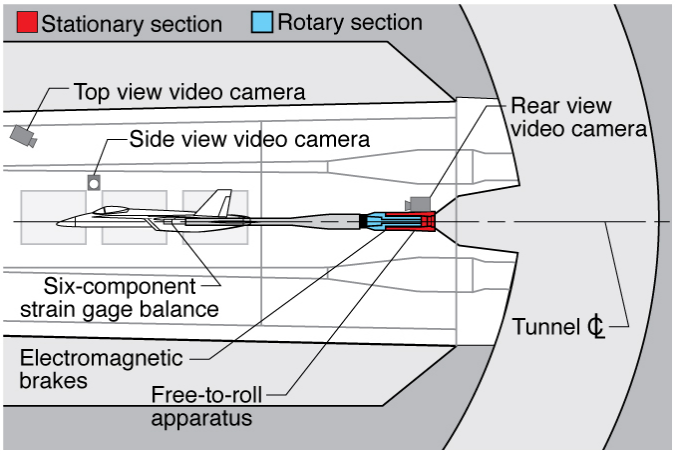

Fig. 21. Sketch of the NASA Langley NTF FTR apparatus.

The FTR test technique is a single degree-of-freedom test method in which the model is free to roll about the longitudinal body axis. The overall objective of FTR testing is an early identification of potential uncommanded lateral motion problems (or lack thereof). If the results of static force and moment tests indicate that a potential exists for wing rock/drop, the FTR method can then be used to study the dynamic behavior. Inherently, the FTR technique evaluates unsteady, non-linear aerodynamics. The technique allows for an estimation of the roll damping derivative, C_{l_p}. In addition to estimates of aerodynamic parameters, if the model and test conditions are appropriately dynamically scaled, estimates of full-scale motions (e.g., amplitudes, frequencies, and accelerations) could be made. Since the FTR tests are designed to be conducted with the same models, and even during the same test entry used for traditional static force and moment measurements, the models do not usually incorporate an active control system to stabilize the motions or duplicate the effects of the stabilization system of the full-scale aircraft.

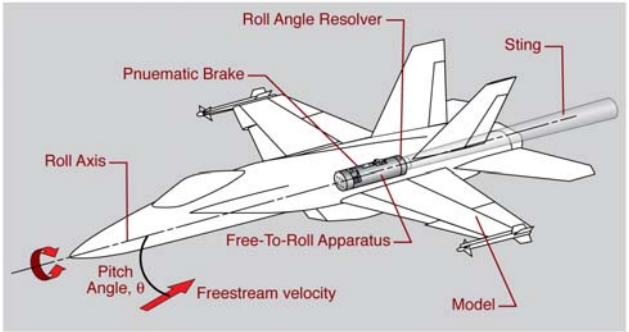

Fig. 22 Internally mounted FTR rig.

Figure 20 shows kinematic relationships during the rolling motion. For a given pitch angle, θ, as the model rolls from a wings-level condition, the angle of attack, α, decreases and angle of sideslip, β, increases in magnitude. The mathematical representations of the kinematics are given as $\alpha = \tan^{-1}(\cos\phi \tan\theta)$ and $\beta = \sin^{-1}(\sin\phi \sin\theta)$. Also, note that for the FTR technique: $p = \dot{\phi}$, $q = 0$, and $r = 0$. As shown in Fig. 20, the down-going wing experiences an incremental increase in α. At the wing tips, this increment is equal to $\tan^{-1}(pb/2V_\infty)$. In a similar fashion, the up-going wing experiences a decrease in α of identical magnitude. If the model is in wing stall conditions, the rolling motion may result in undesirable dynamic behavior. Specifically, at a value of θ in the stall region, the local sectional lift characteristics of the down-going wing might experience a greater loss in lift than the up-going wing. This lift differential would then propel the motion rather than damp the motion and the model would exhibit a loss in roll damping. In other words, the value of C_{l_p} would become positive.

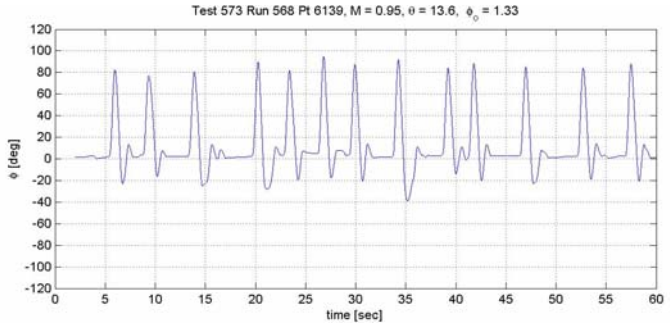

Fig. 23 Roll angle time history demonstrating wing drop

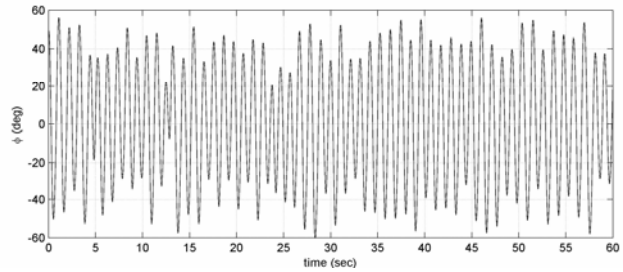

Fig. 24 Roll angle time history demonstrating wing rock

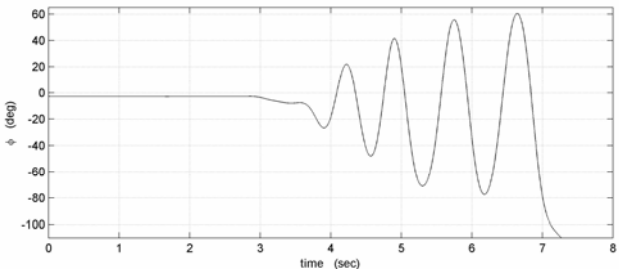

Fig. 25 Roll angle time history demonstrating wing rock divergence.

Governing Equation

The equation of motion for the FTR technique can be represented as: $\frac{I_x \ddot{\phi}}{qSb} + C_{l_{\dot{\phi}}} \frac{\dot{\phi} b}{2V_\infty} + C_{l_\phi} \phi = C_{l_o}$. The governing equation was cast in terms of the Euler angle ϕ since this directly models the FTR motion about the longitudinal body axis. This differential equation can be non-linear because the aerodynamic coefficients can be functions of θ, ϕ, $\dot{\phi}$, $\ddot{\phi}$, time, Mach number, etc. The foregoing equation is in the form of the classical mass-spring-damper system where: C_{l_o} represents an aerodynamic forcing function for ϕ = 0°; C_{l_ϕ} represents the spring constant which, along with the inertia, determines the frequency of oscillation; and $C_{l_{\dot{\phi}}}$ represents the damping coefficient. Note that friction in the system can be accounted for in the damping term.

Since the governing equation for the FTR method contains the static derivative C_{l_ϕ} instead of C_{l_β}, it is advantageous to make ϕ-sweep runs during the static force portion of the test. This allows for a clearer understanding of the static lateral stability that the model experiences while it rolls between some ϕ-range. The C_l vs. ϕ curve will define the steady-state value of C_{l_o}, the non-linearity of the spring, the frequency of the motion, and nominal range of ϕ that the model will oscillate within. If hysteresis is present, then ϕ-sweeps in both directions must be made in order to capture the full non-linearity of the spring.

A sketch of the NTF (formerly, the 16-ft TT) FTR rig is shown in Fig. 21. The design and implementation of the NTF FTR rig is explained in Ref. 24. When the apparatus is in a FTR mode, the rotary section of the FTR rig, the sting, the balance, and the model all rotate on two sets of bearings. This has the unfortunate side effect of significantly increasing the roll inertia which makes dynamic scaling difficult. Electromagnetic brakes can be engaged to stop the motion and to hold the model at an initial roll angle. In order to conduct static force tests, the model can be held in a rigid position by a locking bar placed across the rotary and stationary parts. Switching between the static-force mode and the FTR mode requires about one hour. An alternative to the configuration shown in Fig. 21 is one in which the balance is replaced by a FTR rig (Fig. 22). The advantage to this method is that it greatly reduces the roll inertia making it easier to dynamically scale this parameter. The disadvantage is the longer time to transition between FTR and static force and moment.

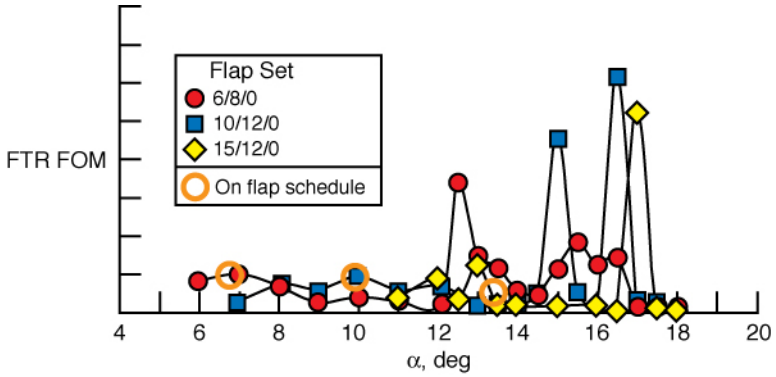

Fig. 26 Example of using the FTR-FOM for LE flap scheduling.

During the free-to-roll phase of the stability and control test, force and moment data is measured using a six-component strain-gauge balance and the roll-angle time history is measured with a resolver. The resolver has an accuracy of 0.067° and the signal is typically sampled at a rate of 50 Hz or higher. This signal is filtered using an analog 4 Hz low-pass Butterworth filter. Also, video of the rolling motions from different views are recorded.

The general procedure for the use of the FTR technique in a stability and control test follows. For a given configuration, a static-force phase consists mainly of α-sweeps and is conducted first. Then, the locking-bar is removed and the FTR phase is conducted. During the FTR phase, three testing methods are utilized: continuous pitch-sweeps, pitch-pause, and bank-and-release. The continuous pitch-sweeps are conducted by slowly pitching the model up through the desired θ-range and then pitching the model back down through the θ-range while the model is free to roll. This method is used to quickly find the θ-range where lateral activity exists, if at all, and permits for an assessment of any hysteresis effects in pitch angle. Various pitch rates are also used to assess pitch rate effects on the development of the uncommanded lateral motions. Following the continuous pitch sweeps, pitch-pause points are taken. Pitch-pause points are taken to assess the lateral activity at specific pitch angles. In this procedure the model is held fixed with the wings level (± 2°) using the brakes. The model is then moved to the desired pitch angle. When on point, the brakes are released and the ensuing motion is recorded. The precursor continuous pitch-sweeps are used to determine over what range of α that finer increments in θ are needed. The pitch-pause points are used to determine the tendencies of lateral motions to develop from a $\phi = 0$ and $\dot{\phi} = 0$ condition. Next, the bank-and-release points are conducted by releasing the model from a $\phi \neq 0$ and $\dot{\phi} = 0$ condition, which induces a rolling motion by the action of the static lateral stability. This procedure will accomplish three objectives: (1) allow assessment of roll damping, (2) discover if the model will develop sustained lateral activity given an initial rolling motion, and (3) determine if the induced rolling motion will impact the lateral activity seen before. After the FTR phase is completed the locking-bar is replaced for additional static force measurements. During this phase, ϕ-sweeps and β-sweeps are conducted in order to quantify the static lateral characteristics. The pitch angles for these sweeps are ones where significant lateral activity was seen during the FTR phase.

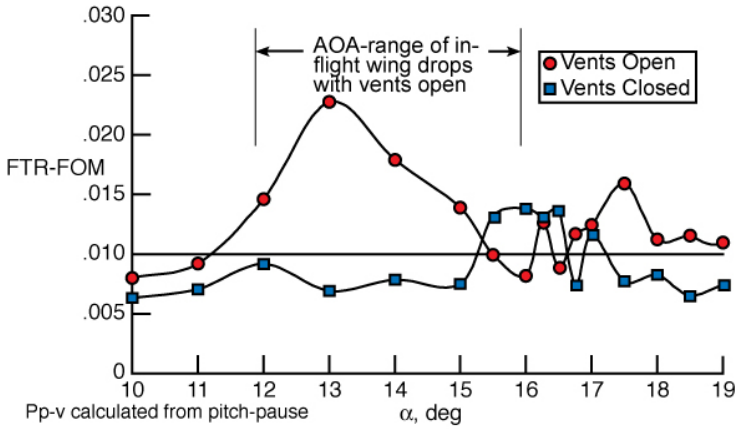

Fig. 27 FTR-FOM showing the effect of LEX vent position for the pre-production F/A-18E. The data also shows the favorable comparison to flight.

One caution regarding the application of the FTR test technique is the use of the method at low pitch angles. During FTR testing, the wings are leveled by the static lateral stability ($C_{l_\beta} < 0$). Recalling the kinematic relationships given earlier, if the model is disturbed from a wings level condition at low pitch angles the model will roll to large bank angles in order to generate enough rolling moment due to sideslip to counter this disturbance. Therefore, at low pitch angles the rolling motions may be difficult to interpret, especially if the model has out-of-trim roll characteristics or if the wind tunnel has significant flow angularity.

The top-level analysis from FTR testing involves assessing the severity of lateral activity (rolling motion). Since the models are typically not dynamically scaled, it is difficult to draw the line between acceptable and unacceptable lateral activity based solely on the behavior of the model. Therefore, the severity of the lateral activity is assessed using the flight data correlated FTR FOM that was developed during the AWS program[14]. The FTR FOM is computed from a time history of the roll angle using the following procedure. First, the absolute value of the amplitude change from a local maximum (peak) to its nearest local minimum (valley) is determined. Then, this value is divided by the time it takes to roll through this amplitude change. This ratio is, of course, the slope of a line connecting the maximum to the subsequent minimum. This quotient is computed for all of the maximums and minimums in a time history, and the final FTR FOM, $p_{p\text{-}v}$, is selected as the highest of these ratios. Mathematically stated as: $p_{P-V} \equiv \left(\left| \frac{\Delta\phi}{\Delta t} \right| \frac{b}{2V_\infty} \right)_{\max}$. This FOM is not intended to indicate the type of motion, how long it took for the motion to develop, or how often the events happened. However, it has proven to be an accurate indicator of where uncommanded lateral motion will occur in flight and serves as conservative first filter for assessing the severity of the motion. Figures 23-25 shows example roll angle time histories of the transonic FTR tests to demonstrate the range of motion and frequencies. Figures 26 and 27 show examples of the application of the FTR-FOM.

In summary, the FTR test technique has been used successfully in the low-speed range for many decades in many facilities around the world. Now the use of FTR in the transonic speed regime is possible in a production mode at both the NTF and Calspan 8-Foot Transonic tunnel. The FTR test technique is used in conjunction with static force and moment testing to access the effect of unsteady aerodynamics on uncommanded lateral activity. The effects of dynamic scaling and friction must be taken into account to accurately understand the results. A FTR-FOM has been developed to guide in the discernment of significant lateral activity.

As stated earlier, the FTR technique is used in conjunction with static force and moment tests. The ideal stability and control test apparatus would be one that could conduct static force and moment, forced oscillation about all three axis (not at the same time necessarily), and FTR without having to remount the model or sting and be able to transition between each technique without stopping the tunnel. A preliminary design of such a rig with oscillation or FTR capability about only the roll axis has been produced for the Transonic Dynamics Tunnel.

Fig. 28 NACA 5-foot Free-flight Tunnel shown rotated to match model glide slope.

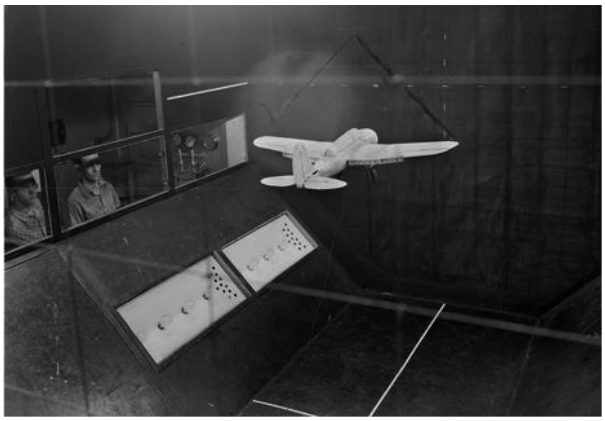

Fig. 29 Testing a 1/12th scale model of SBN-1 in the 12-Foot Free-Flight Tunnel.

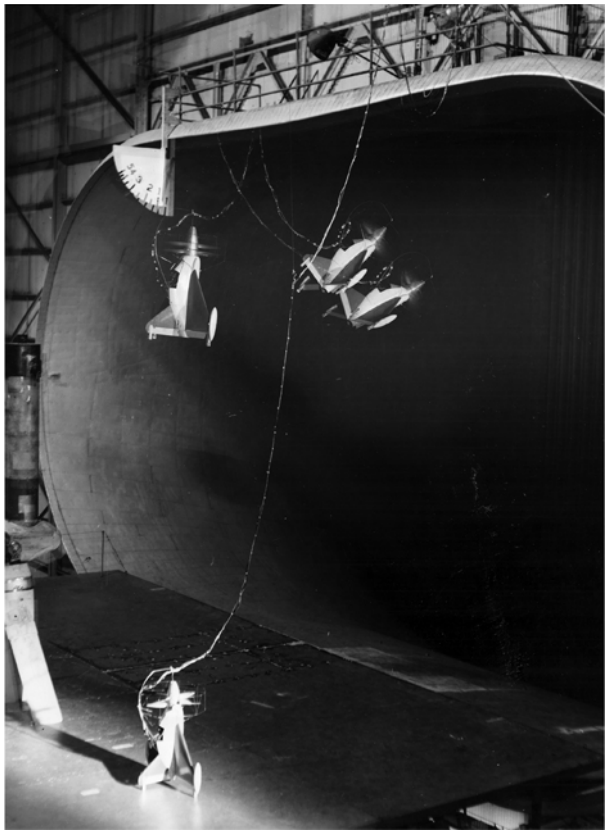

Fig. 30 Multiple-exposure photograph of Convair XFY-1 free-flight test in Langley Full-Scale Tunnel.

VI. Free-Flight

Free-flight testing is a wind tunnel test technique using a remote controlled model flown unconstrained in the tunnel test section. This technique, with a properly scaled model, provides an experimental simulation environment that will closely replicate the motions of the full-scale airplane. Early incarnations of this technique used unpowered models in small tunnels that could be tilted to match the glide slope of the model at a particular air speed. The first of these tilting free-flight tunnels was built at Langley in 1937 with a 5-foot diameter test section (Fig. 28). This was followed two years later by a larger 12-foot diameter free-flight tunnel (Fig. 29). In the early 1950s the free-flight technique transitioned to larger models and the much larger 30 by 60-foot test section of the Langley Full-scale Tunnel (LFST) shown in Fig. 30. Nearly every United States fighter aircraft developed over the next fifty years was free-flight tested in the LFST. In 1998 the free-flight test capability was extended to the Langley 14- by 22-Foot Subsonic Tunnel (14x22) in an effort to maintain the capability after the LFST closed (Fig. 31).

The current implementation of the free-flight test technique, illustrated in Figs. 32 and 33, splits the piloting tasks between a pitch pilot, thrust pilot and roll/yaw pilot. This splitting of the piloting tasks is done for several reasons. As the model scale is reduced, the model dynamics are accelerated requiring a rapid pilot response. The confined test area also requires the pilot to quickly arrest model translations. And finally, since the pilots are remotely located they lack the acceleration cues which can result in some lag in the pilot response. All of these factors result in a high workload piloting task that is mitigated by splitting the tasks amongst the three pilots.

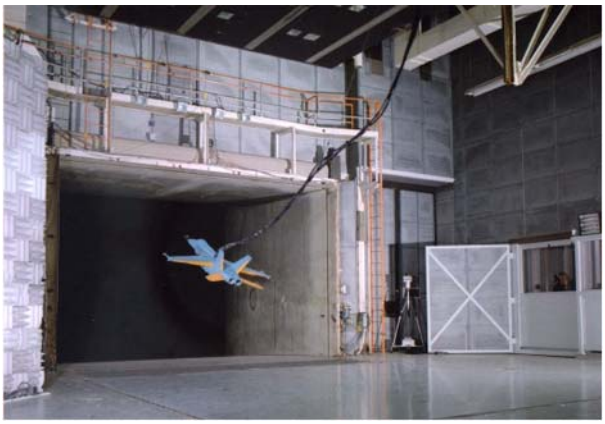

Fig. 31 Free-flight test of 11% scale F/A-18 E/F in Langley 14- by 22-Foot Subsonic Tunnel.

The pitch pilot, thrust pilot and the safety cable operator are stationed to one side of the test section with a good view of the model vertical and longitudinal motions. The roll/yaw pilot is provided a view from behind the model via video cameras located downstream of the test section in the 14- by 22-Foot Subsonic Tunnel (Fig. 32) or a special pilot station located in the exit cone in the LFST (Fig. 33). The models are generally powered by high pressure air that is regulated by the thrust pilot. The high pressure air is supplied to the model via a light flexible cable the also provides electric power and control signals for the control actuators and sensors carried within the model. This cable also includes a 1/8-inch diameter steel safety cable that is used to restrain the model when an uncontrolled motion develops or to terminate the test. The cable is kept slack

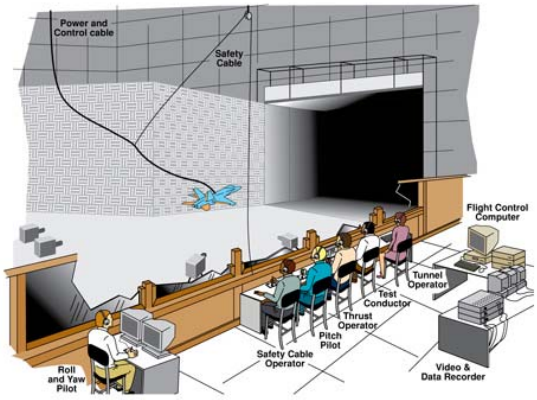

Fig. 32 Free-flight test setup in the 14- by 22-Foot Subsonic Tunnel

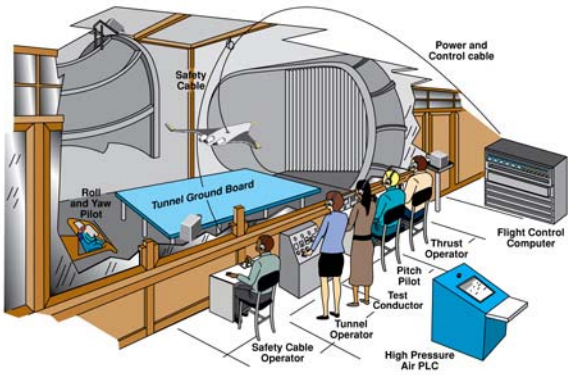

Fig. 33 Free-flight test setup in LFST.

during the test by the safety-cable operator controlling a high-speed winch. The model is flown in 1g level flight through various angles of attack by balancing the thrust and flight controls at various tunnel airspeeds.

An external flight control computer is used to process the aircraft control laws at the feedback rate required by the dynamic scaling relationships. The dynamic scaling relationships are provided in Table 1. Sensors onboard the model are used to measure flight variables and supply appropriate signals for the control laws. Typical sensors include control-position indicators, linear accelerometers, angular rate gyros and boom-mounted vanes for angle of attack and sideslip. High bandwidth electro mechanical actuators are used to position the model control surfaces. Video data is recorded from three cameras positioned about the test section. Sensor and control law parameters are sample and recorded at 200 Hz for post test analysis.

The free-flight models must be dynamically scaled to provide reasonable predictions of full-scale flight dynamics. As seen from the dynamic scaling relationships in Table 1, the larger the model the easier it is to satisfy the mass and inertia scaling requirements. The maximum size of a free-flight model is limited by the size of the tunnel. The wing span of the model should not be more than 1/5 the width of the tunnel. Models that are larger result in insufficient maneuvering space. The mass and inertia scaling requirements along with the model size limits can be very challenging when building free-flight models of large aircraft configurations. An example is the Blended-Wing-Body (BWB) configuration that was recently tested (Fig. 34). This configuration could not be scaled to fit in the 14-by-22-Foot Subsonic Tunnel and meet the mass and inertia requirements. A larger scale model had to be tested in the larger LFST.

The free-flight test technique provides a six-degree-of-freedom, 1g, dynamic flight environment for early evaluation of an aircraft configuration's stability, controllability and flying qualities. The technique is particularly useful in flight regimes that are dynamic or difficult to model such as 1g departures, asymmetric thrust conditions or configuration transitions. The technique has also been used to evaluate flying qualities in dynamic environments such as formation flight or wake encounters as shown in Fig. 35. The tests are conducted in an indoor controlled environment under sustainable and repeatable conditions. This can be particularly useful for classified or proprietary configurations. The technique can also be very productive with multiple configuration and control law modifications quickly implemented and evaluated over a relatively short test period. The free-flight models are often designed for and used in static and forced oscillation test to fully leverage development costs. Free-flight testing can be a cost effective precursor or possible alternative to RPV or full-scale flight testing.

Fig. 34 Free-flight test of a 5% scale BWB in LFST.

The free-flight technique also has its limitations or disadvantages. One of the biggest limitations is Reynolds number scaling. The technique is conducted in atmospheric tunnels at low dynamic pressures with small scale models. The test Reynolds number is generally significantly lower than full-scale and can lead to prediction errors. The technique is also limited to 1g maneuvers. Accelerated stalls or high g maneuvers cannot be tested. Rapid speed changes such as those during VSTOL transitions are difficult to test and are limited by the generally slow speed response of the tunnel. Safety cable effects, although generally minimal, can sometimes affect the models response. As previously noted, the dynamic scaling mass and inertia requirements can be very challenging as the scale of the model is reduced. The free-flight technique also requires a unique skill set amongst the pilots to not only control but assess the flying qualities of the models. This skill set is difficult to maintain with fewer test articles for the reduced number of airplanes being developed today.

Fig. 35 Free-flight wake encounter test in LFST.

VII. Free Spin/Free Fall/Free Tumble

As with the rotary and combined motion tests described earlier, free-flying tests of dynamically scaled models are conducted in the 20-Foot Vertical Spin Tunnel (Fig. 15). The data acquisition system used with free-flying models (i.e., "MSPS") will be described later in this section.

Free-Flying Models

As noted earlier in this paper, the dynamic scaling technique allows motions of free-flying models to be scaled up to predict full-scale behavior by preserving dynamic similitude (i.e., equal Froude number and relative density, μ_{rel}) between the model and full-scale vehicle. However, practical considerations[5] make providing dynamic scaling in conjunction with Mach or Reynolds number similitude difficult. Since the VST is a low-speed atmospheric tunnel, Mach and Reynolds number similitude are not satisfied unless the full-scale vehicle happens to operate at the low Mach, low Reynolds number conditions of the facility. Dynamically scaled models used in the VST typically have a length (e.g., wing span, capsule maximum diameter, etc.) on the order of 12 to 24 inches.

Model control surfaces (if applicable) are actuated using premium off-the-shelf remote control (R/C) hobby gear (i.e., transmitter, receiver, servos, batteries, etc.) in an open-loop fashion. Deflections for the spin attempt and spin recovery are pre-programmed by the test engineer into the transmitter prior to each test run, and checked against "protractors" that measure trailing-edge deflection (usually with respect to the hinge line) that are custom built for each model. Servos are sized for both torque and slew rate to ensure full and rapid deflection of the control surfaces from their pro-spin deflections to their recovery deflections.

Fig. 36 Spin model on swing rig.

As depicted in Fig. 15, a lightweight "safety tether" attached to a small, high-speed electric winch is sometimes used during testing to minimize damage by preventing models from impacting the test section walls or netting. The tether is attached to a model near its center of gravity with a ball-bearing swivel and is kept slack by a winch operator during a test unless model impact is imminent. Unpublished tests have shown that the tether has a negligible effect on the dynamic behavior of models under test.

Determining mass properties of free-flying models

A critical step in preparing a dynamically scaled model for testing is precise measurement of its mass properties. A Space Electronics™ "swing rig" (Fig. 36) at the VST is used to measure model center-of-gravity location and moments of inertia about each body axis[27]. After initial measurement of a model's c.g. and moments of inertia, a simple algorithm that utilizes a point-mass assumption is run to estimate any ballast required. The model is then re-swung in an iterative process until the target full-scale mass properties are satisfied. Models are routinely re-swung throughout a test either to ensure that inadvertent damage has not altered the mass properties, or to re-ballast to a new test condition.

Fig. 37 Free-spin test of dynamically-scaled fighter model in VST.

Data acquisition and processing

The Model Space Positioning System (MSPS)[28] is a video-based system that stores digital images of free-flying models for post-test determination of attitude, position, and rates. Up to four analog charge-coupled-device (CCD) cameras (one of the four is depicted graphically in Fig. 15) provide input into the system to give maximum test section coverage. The system is based on Tau Corp.'s Eagle™ tracking system and resides on a UNIX workstation. Scientific-grade digital optical disks are used as storage media. Retro-reflective targets with precisely-measured centroids relative to the model body axis system are imaged by the system during the test. After acquisition and image storage, a "pose estimation" algorithm is used to iteratively estimate (by minimizing the error between the model, or

more precisely *target*, images and the numerical best-fit solution until an "acceptable" level is reached) model attitude and location in the test section at up to 1/60-s time intervals from any single camera view. As such, the system is not based on photogrammetry in which stereoscopic views of an object are triangulated. Parameters estimated by the system are model roll, pitch, and yaw angles (ψ, θ, and ϕ) and x, y, and z position of the model reference center relative to the tunnel reference system. Rates are calculated by numerically differencing time histories of the angles and spatial coordinates. These cameras provide 60-Hz imaging of retro-reflective targets that are precisely positioned on the surface of the model relative to any appropriate reference system. Time history data from this system is often used to benchmark and calibrate high-fidelity six degree-of-freedom (6-DOF) simulations of aircraft and atmospheric entry vehicles. Angular accuracies are within ±1 degree of a known reference, although values closer to ±0.5 degree are typical. NASA Langley is currently in the process of upgrading this system to provide significantly higher frame rates and image resolution for improved accuracy.

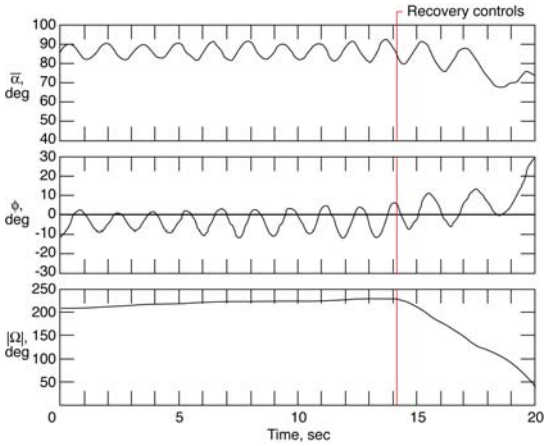

Fig. 38 Typical spin time history using MSPS data system in VST.

Free-spin and free-tumble testing

One of the most common uses of dynamically scaled models in the VST is for identification and analysis of airplane spin modes and spin-recovery characteristics (e.g., Ref. 29), including size requirements for emergency spin recovery parachutes (Fig. 37). Spin models are hand launched with pre-rotation in a high angle of attack condition into the vertically rising air stream. The tunnel operator adjusts test section velocity to match the sink rate of the model. If a spin mode or modes exist, the model attitude and spin rate will tend to settle in to a steady state (or oscillate about mean values). An example of a time history trace (as measured by MSPS) from a free-spin test is shown in Fig. 38, where a model's pitch angle, roll angle, and spin rate magnitude are plotted versus time (converted to full-scale using the dynamic scaling laws). The spin depicted is "locked in" but oscillatory, i.e. the pitch and roll angles oscillate about a mean value. Note that the spin rate did not completely level out until approximately 10 seconds into the test. At approximately 13.2 seconds into this test, the recovery control command was initiated by sending a signal from the radio transmitter to the model's on-board receiver, which commanded servos to drive the control surfaces to their pre-determined recovery deflections (indicate by the vertical bar), resulting in the spin rate beginning to bleed off and the pitch and roll angles deviating significantly from the those during the "steady" spin. The number of turns for recovery was determined by review of documentation video.

Fig. 39 Dynamically-scaled sample return capsule model in VST.

Tumble tests of flying-wings[30] or other non-conventional configurations are accomplished in a manner very similar to free-spin testing. Since a tumbling model creates net lift and thus does not have a vertical flight path like a spinning model, the tests are usually of short duration as the model traverses the test section. When longer test times are desired, a "free-to-pitch" rig is used. This rig allows a model to rotate about the pitch axis only (1-DOF), but provides test times of any desired length.

Entry vehicle testing

Another type of testing uniquely suited to a vertical tunnel is dynamic stability testing of atmospheric entry vehicles at subsonic conditions, as well as drogue parachute performance and interactions of the parachute with the wake of the vehicle. Models of both manned and unmanned vehicles have been tested at the VST over the years, from the Mercury, Gemini, and Apollo programs and planetary probes (e.g. Pioneer Venus) to current sample return spacecraft such as Stardust[31] and proposed missions to the Moon and Mars. An example of a prototype sample

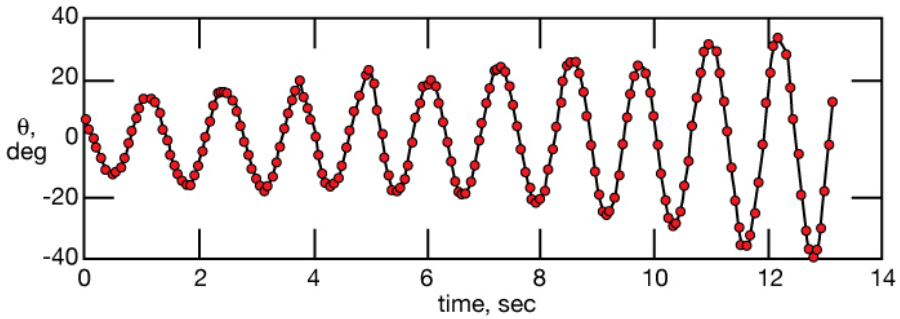

Fig. 40 Dynamic response of statically-stable sample return capsule model to perturbation in VST.

return vehicle is shown in Fig. 39. By manually perturbing the attitude of a free-flying model, qualitative determination of the tendency for oscillations to damp out, settle into a limit-cycle, or continually increase in amplitude can be made. In Fig. 40, a sample time history of a certain model's response to a perturbation shows that the oscillation amplitude grows with time even though the configuration is statically stable. Using parameter identification (PID) methods in conjunction with time history data from the MSPS allows quantitative estimation of a configuration's dynamic damping derivative values for implementation into a simulation[32].

VIII. Drop Model/UAV

This section describes the outside free-flying test techniques – drop model and UAV. Aeronautical research requires flight testing, both for validation of results obtained on the ground, and to guide the research itself. In general, the more complex the research issues, the more flight testing that must be done to get reliable answers. For some research, such as flight testing involving spins or out-of-control motion, or developing reconfigurable control under failure conditions, it is impractical to use manned aircraft for flight research because of high costs and safety risks. There is also a need for an intermediate step between simulation and full scale flight testing, particularly for nonlinear dynamic modeling and novel control designs. A subscale model aircraft can provide increased confidence in the methods and developments before risking the large investment ultimately necessary for full scale flight test demonstration. Since subscale flying models are less expensive and unmanned, risks can be taken in research and development that could never be tolerated in a piloted flight test. NASA Langley Research Center (LaRC) has a long history of using subscale aircraft for flight research, and currently is heavily invested in using subscale aircraft for flight research.[33-35] By adhering to the appropriate scaling rules, these model techniques enable accurate predictions of flight dynamics across a wide range of flight phenomena that are difficult if not impossible to ascertain in any other way.

Although both the drop model and UAV techniques use remotely piloted vehicles (RPV) the differences between the two are dictated by the scope of the research. The models used in the helicopter drop testing are generally unpowered, launched from a carrier vehicle, and recovered by parachute to avoid take-off and landing risks. The drop models are typically quarter-scale in order to house the flight systems and meet dynamic scaling parameters. The UAV typically has a wing span of no greater than 10 feet and takes-off and lands under its own power. These techniques can be used to study maneuvering flight. For an example, the RPV is maneuvered from a straight and level flight condition to imminent stall, stall, post-stall, imminent spin, fully-developed spin, spin recovery then back to straight and level flight. Like the tunnel-based free-flight models the outdoor free-flying models are dynamically scaled and extensively outfitted with high fidelity instruments to measure aircraft states, air data, and flight systems health. As such, the motions resulting from a wide variety of unconstrained flight conditions can be thoroughly analyzed. These data are often the sole source of information to formulate flying qualities predictions of highly dynamic conditions. Moreover, the aircraft-state time history data from such tests can be used to update and validate simulation models. The recent advancements in the miniaturization of quality electronics have greatly reduced the sizing and weight impact of integrating model instrumentation. The models are flown at NASA/FAA approved airports and the NASA Wallops Flight Facility.

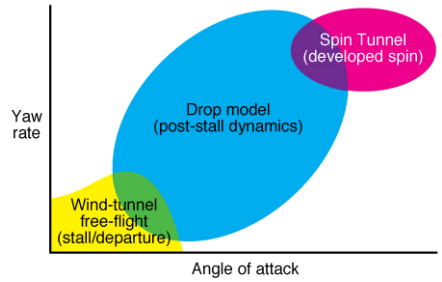

Fig. 41 Region of flight dynamics addressed by the drop model technique

Drop model

Figure 41 shows that a significant void of information exists between the pre-stall and stall departure results produced by the wind tunnel free-flight tests and the fully developed spin behavior observed in the spin tunnel tests. The radio-controlled drop model technique was originally developed in the 1950's to fill this void, providing information on the post-stall and spin-entry motions of airplanes. With the need to provide combat aircraft with the capacity to aggressively maneuver at and beyond stall, the drop model technique has been further developed to permit the investigation of the related flight dynamics issues while the test configuration is undergoing large amplitude, high rate maneuvers over the entire low-speed flight regime and is not solely focused on spin entry. For example, past drop model programs of various aircraft configurations have explored a variety of low-speed phenomena including highly dynamic motions such as divergent wing-rock, aggressive tumbling, and roll departures as well as more docile areas such as pitch control enhancement, parameter identification, and control law refinements for accelerated and

Fig. 42 Drop model just released from helicopter.

Fig. 43 Drop model cockpit

unaccelerated stability improvements.[1-3] The overall operation of the helicopter drop-model technique involves dropping an unpowered, dynamically scaled model from altitude (Fig. 42), flying it through a series of maneuvers by remote control from the ground, and recovering it with a flight termination parachute. To meet dynamic scaling requirements the typical helicopter drop models are generally near quarter-scale and weigh 500 to 1200 lbs. The model is dropped from altitudes of up to 15,000 feet and is tracked by a manually operated ground-based tracker on which video cameras, a radar ranging system, and telemetry antennas are mounted. The equivalent airplane altitude depends on the model scale factor, the model-to-airplane mass ratio, and the air density: for example, 15,000-ft model altitude is about 35,000-ft full-scale equivalent for the F/A-18E/F. A camera is mounted in the canopy of the model to provide an onboard-pilot's view. The pilot sits at a control station and monitors data displays and the video images while providing three-axis control through a customized cockpit as shown in Fig. 43. The overall control loop consists of down-linked flight data, a digital computer on which the control laws are implemented, and a command uplink. Once the pilot has executed the intended profile, the onboard flight termination parachute is deployed to decelerate the model for landing. The drop model carries an extensive complement of flight instrumentation to provide real-time state feedback information to the flight control computer, to drive real-time data displays for the ground-based pilot, and for post-flight data analysis. Duplex flight sensors measure angle of attack, sideslip, airspeed, 3-axis angular rates and linear accelerations, and 3-axis attitude. Simplex flight instruments include pitot and static pressures, radar range, pilot's-eye-view video, and control surface position transducers. Various system-monitoring parameters and all of the flight sensor signals are down-linked to a ground-based data logging system and, along with pilot comments, video imagery from the ground, and digital recordings of ground-generated signals (such as pilot commands and mode selections) form the collection of data obtained during a flight.

Fig. 44 ARES model balloon lift

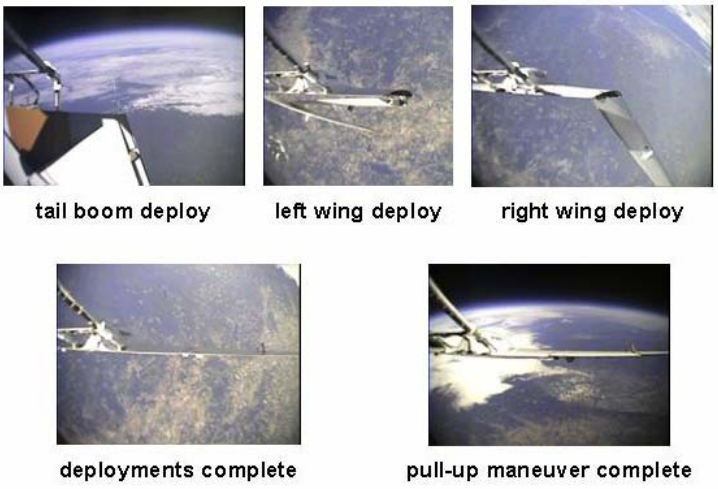

Fig. 45 Sequence showing the deployment of the ARES from the balloon to the completed pull-up maneuver.

Drop model testing has proven to be instrumental in areas other than post-stall dynamics. A recent use of the outdoor flying test method has been focused on validating low angle-of-attack CFD-based performance predictions for an atypical flight environment. The proposed space mission known as Aerial Regional-scale Environmental Survey (ARES) involves flying an airplane at 1.5-kilometer altitude over the surface of Mars to conduct scientific investigations that are unachievable with landers, rovers, or orbiters (Ref. 36). To enable the science, the airplane must transform from its folded space-transport configuration into a flying airplane platform, and it must do so during the descent through the Mars atmosphere. The conditions at Mars are

characterized by temperatures 100 degrees F colder and densities 100 times lower than those at sea-level on Earth. These environments drive the flight envelope to relatively high Mach number and relatively low Reynolds number conditions – a rare combination that is relatively unexplored and is typically only found on Earth well into the stratosphere.

Flying a model at about 100,000-foot altitude over Earth enables studies of the aerodynamic properties relevant to flight over the Martian landscape, a key consideration for the ARES program. Reaching the 100,000-foot level can be easily achieved with helium balloon lift technology. The basic operation of the balloon drop model technique involves suspending the appropriately scaled model at the end of the balloon train, allowing it to ascend uncontrolled to the proper altitude where it is released on command and flown autonomously by the onboard flight control computer. The autopilot makes use of GPS, three-axis accelerometers, magnetometers, three-axis rates, and a multi-hole air data system to drive the actuators so the vehicle performs its pre-defined maneuvers and executes its waypoint navigation. Once the model descends below about 1000 feet, a ground-based pilot overrides the auto-navigation algorithm for a runway landing directly on the model belly (the ARES Mars variant will not be required to perform a soft landing and therefore has no landing gear).

The 50%-scale model of the ARES design, pictured folded below the 141,000 ft^3 balloon in (Fig. 44), has a mass of 22 kilograms and is completely self sufficient for the autonomous operations. All onboard systems are designed to operate in the cold, low-pressure environment. Important data parameters are telemetered to the ground, but the flight control computer also performs data logging throughout the long ascent and descent. Additionally, a video camera, mounted to the right tail, provides a view of the flight. A sequence from this vantage shows the unfolding transformation into an airplane, and includes a view as the wings approach the completion of the pull-up maneuver (Fig. 45). Results from this test aided in the refinement of parametrics needed for additional computationally-based predictions in the low-Reynolds number, high subsonic Mach regime.

Drop model testing provides the means to study a variety of phenomena, from highly dynamic maneuvering to relatively benign maneuvers in unusual environmental conditions. The relevance of the technique relies on achieving similitude in areas of importance to the specific investigation.

UAV

UAVs in use at NASA Langley span the complexity spectrum. One current UAV project[34] utilizes a near zero-cost foam airframe coupled to a hobby-style engine for conducting advanced controls research. This project utilizes as much commercial-off-the-shelf and hobby-style equipment as possible. For added cost efficiencies, wind-tunnel and flight tests have been conducted using the same airframe. Due to the simplicity of the components and their relatively low costs this project has conducted hundreds of flight tests in the span of only a few years. The evidence of the low-cost high-quality nature of the research can be seen in the numerous UAV projects that are being conducted by numerous small businesses and universities. Though effective, these projects typically use non-dynamically scaled test articles and must remain cognizant of the limitations this brings. For example, the low mass moment of inertia typically associated with non-dynamically scaled vehicles gives rise to enhanced maneuvering performance uncharacteristic of the vehicle being represented; yet the non-dynamically scale model can provide insight into trimmed flight performance. On the other end of the complexity spectrum, another current UAV project[33] utilizes a jet-powered, custom built, dynamically scaled model with custom instrumentation. Since the costs associated with this model are significantly high, a pilot training program is in place to reduce the operational risks. Ground support and flight ops require a number of very experienced personnel. This project has a ground station similar to the helicopter drop-model one shown above that serves as the flight station as well as a flight-team training venue to ensure direct familiarity with day-of-flight human interfaces. Current electronic sensor and control technologies enables affordable high quality flight research using subscale models and has given rise to a large number of small UAV projects across the nation.

Regardless of the complexity, the basic tenet of the outside free-flying technique is the ability to conduct flight research with a completely unconstrained model. These techniques enable accurate predictions of flight dynamics across a wide range of flight phenomena that are difficult if not impossible to ascertain in any other way.

IX Dynamic Test Techniques Used to Characterize the Flight Dynamics of the Blended Wing Body

A recent series of tests on a BWB configuration serves as an example of how these various dynamic test techniques are applied. Although this paper will not discuss it in detail, NASA has also in the past five years put a model of the Boeing 757 through a battery of dynamic test techniques in support of the current NASA Aviation Safety Program. NASA has been testing a BWB configuration with Boeing Phantom Works over the past six years. The initial test of the configuration was a free spin and tumble test of a 1.1% dynamically scaled model with actuated control surfaces in the VST (Fig. 46). The objectives of these tests were to:

1. Quantify equilibrium spin and spin-recovery characteristics
2. Quantify equilibrium tumble and tumble-recovery characteristics
3. Determine requirements for a single parachute configuration that would provide both emergency spin and tumble recovery. Note: this emergency parachute system is only required for the experimental flight testing that puts the aircraft at greater risk than intended normal operations.

Fig. 46 1.1-percent dynamically-scaled BWB model undergoing free-spin tests in the VST.

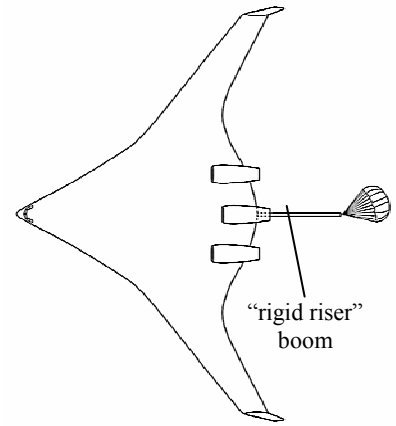

Fig. 47 Sketch of spin- and tumble-recovery parachute developed during dynamic model tests in VST.

Fig. 48 The 21-foot span X-48 UAV undergoing static tests in the Langley Full-Scale Tunnel (note rigid riser boom behind the center engine nozzle.

All of the primary objectives were met during this series of tests, although practical limitations of ballasting the 1.1-percent scale model to the projected flight conditions of the vehicle prevented testing of all desired mass and inertia cases during the free-spin and free-tumble tests (objectives 1 and 2). For this series of tests, equilibrium spin and tumble modes were identified but only when pro-spin and tumble control deflections were used in conjunction with certain mass properties. These combinations of mass properties and control deflections were used to determine requirements for an emergency spin and tumble recovery parachute system. Numerous combinations of canopy size, towline (i.e., riser plus suspension line) length, number of parachutes used, and attachment point location (trailing edge, one or both wing tips, etc.) were tested before arriving at a final configuration. For example, it was determined that both single and dual wing tip mounted chutes provided very good spin recovery, but were unsatisfactory for tumble recovery due to their tendency to foul on the wings and winglets. Therefore a parachute with a very short towline attached to a boom, or "rigid riser"[37], extending off the rear of the model along the centerline was proposed and tested (Fig. 47). This arrangement allowed the parachute to perform satisfactorily for arresting both spins and tumbles. The short towline permitted the canopy to clear the aft end of the model, including the center engine nacelle, as the model pitched through a 90 degree nose-high attitude during a tumble while still

providing good spin recoveries. The boom increased the moment arm (in yaw and pitch) available for the drag forces produced by the parachute to act through, allowing a significantly smaller parachute to be used relative to more standard spin chute installations. The tests were conducted with a fixed length riser attached to the model with the assumption that the flight test vehicle would use some type of extendable or deployable boom. Based on the results of this test, a scaled-up version of the boom-mounted parachute is being incorporated into a flight-test UAV

Fig. 49 The 3-percent scaled BWB model post-mounted undergoing static tests in the 14- by 22-Foot Subsonic Tunnel.

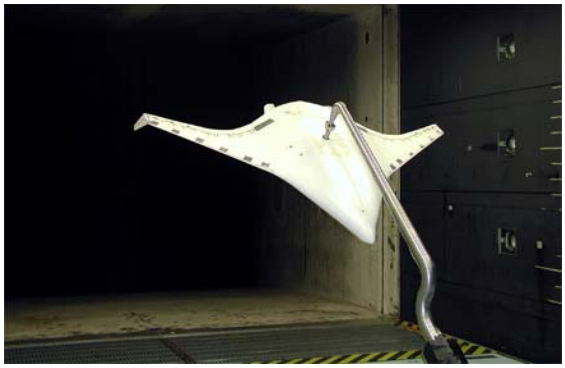

Fig. 50 The 3-percent scaled BWB model bent-sting mounted undergoing large angle static tests in the 14- by 22-Foot Subsonic Tunnel.

(X-48B, Fig. 48). This UAV will be used to investigate flying qualities and flight dynamic characteristics of the vehicle.

The bulk of the low-speed aerodynamic database was developed from a series of tests with a 3-percent scale multi-purpose model. The basic static aerodynamic data was collected in the Langley 14- by 22-Foot Subsonic Tunnel on a post mount system (Fig. 49). A second entry on a bent-sting mount (Fig. 50) was used to collect static data at large angles - ±180° angle-of-attack and ±90° of sideslip. The third entry in this facility with this model was a forced oscillation test to measure damping derivatives about all three axes (Fig. 51). Also, a rotary balance test of a 2-percent scale BWB configuration was conducted in the VST (Fig. 52). The objective of this test was to measure forces and moments under steady rotation for a large range of angles of attack, sideslip, and rotation rate. The large-angle static data along with the forced oscillation and rotary data are all part of the information set required to simulate spins, tumbles and recoveries from other extreme attitudes. The sufficiency of this data set to accurately model and simulate such dynamic maneuvers is an area of ongoing research. Control laws were developed from the aerodynamic data provided from these low-speed tests. These control laws as well as control limits and alternative control effectors were evaluated through a free-flight test in the Langley Full Scale Tunnel with a dynamically scaled 5-percent model as previously shown in Fig. 34. The free-flight test demonstrated the asymmetric thrust

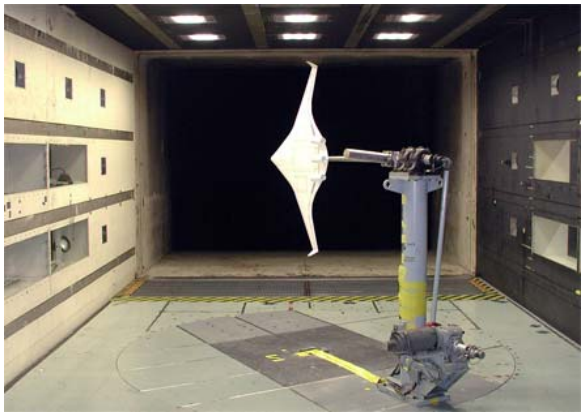

Fig. 51 The 3-percent scaled BWB model undergoing forced-oscillation tests in the 14- by 22-Foot Subsonic Tunnel.

Fig. 52 The 2-percent scaled BWB model undergoing rotary balance tests in the VST.

control limits as well as the potential improvement in those limits with center engine thrust vectoring. The control laws and limits will be further tested in flight with the X-48B. One of the two X-48B vehicles was tested this past May in the Langley Full Scale Tunnel (Fig. 53) prior to shipment to NASA Dryden for flight testing. The wind tunnel test was conducted to validate the vehicle aerodynamics, calibrate the air-data system and measure control surface hinge moments.

Fig. 53 The 21-Foot Span X-48B UAV undergoing static balance tests in the Langley Full-Scale Tunnel.

X. Summary

An overview of various dynamic test techniques used at NASA Langley Research Center on scale models to characterize the flight dynamics of aerospace vehicles was presented. Dynamic test techniques are used in the 12-Foot Low-Speed Tunnel, 20-Foot Vertical Spin Tunnel, 14- by-22-Foot Subsonic Tunnel, National Transonic Facility, Transonic Dynamics Tunnel, Unitary Plan Wind Tunnel, various flying fields and the NASA Wallops Flight Facility. The dynamic test techniques discussed in this paper are forced oscillation, rotary balance, free-to-roll, free spin/tumble/falling, free-flight, drop model and UAV. The paper discussed dynamic scaling to address the similitude requirements for dynamic testing. This section demonstrated that for flight dynamic issues Froude scaling is desired over Mach scaling. An analysis of scaling parameters showed that if the aerodynamic model is well understood then it is possible to scale some of the results from a non-dynamically scaled model test. However, the analysis showed that none of the results can be scaled if a good math model of the aerodynamics does not exist.

The forced oscillation section reported that the low-speed and high-speed techniques that were designed back in the 1950s are still in use today. Although the fundamental concepts are the same since the 1950s, these techniques have received substantial upgrades in both hardware and data acquisition. Additional forced oscillation rigs have been designed and built for the 12-ft LST and VST. These new rigs are either hydraulically or electromechanically driven by computer control so that arbitrary motion can be imparted to the model. This capability provides increased flexibility (e.g. testing at sideslip, arbitrary motion, etc) and test efficiency (e.g. MDOE, Schroeder sweeps, etc.). The forced oscillation section also demonstrated the difficulty in reducing the time history data in the presence of unsteady aerodynamics. Future developments in this area include a multi-degree of freedom rig for the 14-by-22-Foot Subsonic Tunnel.

The rotary balance and combined motion section reported that a forced oscillation capability is being implemented on the VST's rotary rig so that oscillatory coning motion can be studied. Measuring the aerodynamic forces and moments under this motion will provide aid in simulating complex maneuvers and out-of-control modes such as oscillatory spins.

The free-to-roll section reported that the technique has been matured for the transonic regime, and it is possible to predict full-scale aircraft uncommanded lateral motion using an appropriate figure of merit coupled with the static force and moment results. This section stated that the issues with the technique are friction and dynamic scaling. Future plans for the technique involved coupling the technique with the static force & moment and forced oscillation techniques on a single rig. This single rig will allow transition from one technique to the other without tunnel entry or model changes.

The free-flight technique originated in the 1930's in the NACA 5-Foot Free-flight Tunnel and the 12-Foot Free-flight Tunnel (which is still in use today but without the free-flight technique) before transitioning to the 30 X 60 Foot Tunnel (now the Langley Full-Scale Tunnel). NASA abandoned the use of the 30 X 60 Foot Tunnel in 1995 so the free-flight technique was transitioned to the 14-by-22-Foot Subsonic Tunnel. The technique is particularly useful in flight regimes that are dynamic or difficult to model such as 1g departures, asymmetric thrust conditions or configuration transitions. The technique has also been used to evaluate flying qualities in dynamic environments such as formation flight or wake encounters. Free-flight testing can be a cost effective precursor or possible alternative to RPV or full-scale flight testing. Dynamic scaling is a real challenge for the free-flight technique since wind tunnel size limits the size of the model. The larger the model the easier it is to dynamically scale the model. When a Blended Wing Body model free-flight test was proposed the dynamic scaling issues drove the model size such that the 14-by-22-Foot Subsonic Tunnel could not accommodate the model. Therefore, the free-flight technique had to be resurrected in the Langley Full-Scale Tunnel. It was the largest free-flight model ever flown in the Langley Full-Scale Tunnel.

Tests of dynamically scaled, free-flying models have been conducted in the VST since the mid-1930s. Specifically the techniques used are the free-spin, free-tumble, and free-fall technique. The techniques are used on a wide range of aircraft types and planetary entry vehicles. The VST was instrumental in the Mercury and Apollo programs to study the dynamics of the command modules and launch escape vehicles during re-entry or abort modes, respectively. The VST is poised to play a prominent roll in the current design of the Crew Exploration Vehicle. To study recovery techniques, the models are dynamically scaled and have remotely controlled surfaces. The data acquisition system provides attitude time histories from which rates and accelerations can be derived. These techniques use unconstrained models so that the model dynamics from unsteady aerodynamic forces and moments in the absence of support interference can be studied.

As with the other techniques, the outside remotely piloted techniques - drop model and UAV - are not new, having been used for decades at LaRC. What has evolved over the years is the sophistication of the onboard electronics, the amount of data that can be telemetered, and the use of GPS for guidance and navigation. The section

reported an alternate lifting method for the drop-model technique where helium balloons are used to launch the vehicle from the requisite launch altitude of over 100,000 ft.

An example was given that showed how the various dynamic test techniques were used to determine the flight dynamic characteristics and to develop a spin and tumble recovery system for the remotely piloted Blended Wing Body vehicle, X-48B.

Acknowledgments

This paper represents only a small amount of the work that has been done to develop and maintain the dynamic test techniques at NASA LaRC. Although the paper only lists six contributing authors the list could include most of the current and past members of the Flight Dynamics Branch at NASA LaRC.

References

[1]Croom, M.A., Whipple, R.D., Murri, D.G., Grafton, S.B. and Fratello, D.J., "High-Alpha Flight Dynamics Research on the X-29 Configuration Using Dynamic Model Test Techniques," SAE 881420, Aerospace Technology Conference and Exposition, October 1988.

[2]Croom, M.A., Kenney, H.M., Murri, D.M. and Lawson, K.P., "Research on the F/A-18E/F Using a 22% Dynamically-Scaled Drop Model," AIAA 2000-3913, Atmospheric Flight Mechanics Conference and Exhibit, August 2000.

[3]Croom, M.A., Fratello, D.J., Whipple, R.D., O'Rourke, M.J., and Trilling, T.W., "Dynamic Model Testing Of The X-31 Configuration For High-Angle-of-Attack," AIAA 93-3674-CP, August 1993.

[4]Chambers, Joseph R., "Use of Dynamically Scaled Models for Studies of the High-Angle-of-Attack Behavior of Airplanes," International Symposium on Scale Modeling, Tokyo, Japan, July 1988.

[5]Wolowicz, Chester, H.; Bowman, James, S.; and Gilbert, William, P.: Similitude Requirements and Scaling Relationships as Applied to Model Testing. NASA TP-1435, August 1979.

[6]Weber, Ernst: *Physical Units and Standards. Handbook of Engineering Fundamentals*, Ovid W. Eshbach and Mott Sounders, eds., Third ed., John Wiley & Sons, Inc., c. 1975, pp. 385-427.

[7]Croom, Mark A.: "Flight Dynamics Investigations of Large Scale Motions," George Washington University Masters Thesis, August, 2004.

[8]Tomek, D., "The Next Generation of High-Speed Dynamic Stability Wind Tunnel Testing," AIAA-2006-3148, 25th AIAA Aerodynamic Measurement Technology and Ground Testing Conference, June 2006.

[9]Brandon, J.M.: Dynamic Stall Effects and Applications to High Performance Aircraft. Special Course on Aircraft Dynamics at High Angles of Attack: Experiments and Modeling. AGARD Report No. 776, April 1991.

[10]Kim, S., Murphy, P.C., and Klein, V.: Evaluation and Analysis of F-16XL Wind Tunnel Data from Static and Dynamic Tests. NASA TM-2004-213234, June 2004.

[11]Murphy, P.C., and Klein, V.: Validation of Methodology for Estimating Aircraft Unsteady Aerodynamic Parameters from Dynamic Wind Tunnel Tests. AIAA 2003-5397, August 2003.

[12]Chambers, J. R. and Grafton, S. B., "Static and Dynamic Longitudinal Stability Derivatives of a powered 1/9-Scale Model of a Tilt-Wing V/STOL Transport," NASA-TN-D-3591, May 1966

[13]Chambers, J. R. and Grafton, S. B., "Investigation of Lateral-Directional Dynamic Stability of a Tilt-Wing V/STOL Transport," NASA-TN-D-5637, February 1970

[14]Brandon, J. M. and Foster, J. V.: Recent Dynamic Measurements and Considerations for Aerodynamic Modeling of Fighter Airplane Configurations, AIAA-98-4447, August 1998

[15]Wang, Z.; Lan, C. E.; and Brandon, J. M.: Unsteady Aerodynamic Effects of On the Flight Characteristics of an F-16XL Configuration, AIAA-2000-3910.

[16]Heim, E. H. D., and Brandon, J. M., "Uncertainty-Based Approach for Dynamic Aerodynamic Data Acquisition and Analysis," AIAA-2004-5364, August 2004

[17]Zimmerman, C. H.: Preliminary Tests in the N.A.C.A. Free-Spinning Wind Tunnel, NACA TR-557, 1935.

[18]Wenzinger, C., and Harris, T.: The Vertical Wind Tunnel of the National Advisory Committee for Aeronautics, NACA TR 387, 1931.

[19]Bamber, M. J.; and Zimmerman, C. H.: Spinning Characteristics of Wings. I. –Rectangular Clark Y Monoplane Wing, NACA TR 519, 1935.

[20]Bamber, M. J.; and House, R. O.: Spinning Characteristics of the XN2Y-1 Airplane, NACA TR 607, 1937.

[21]Bihrle, W.; and Barnhart, B: "Spin Prediction Techniques", AIAA paper 80-1564, 1980.

[22]Kay, J.: "Acquiring and Modeling Unsteady Aerodynamic Characteristics", AIAA paper 2000-3907, 2000.

[23]Hall, R., and Woodson, S., "Introduction to the Abrupt Wing Stall (AWS) Program," *Journal of Aircraft*, Vol. 41, No. 3, 2004, pp. 425-435.

[24]Capone, F., Owens, B., and Hall, R., "Development of a Free-To-Roll Transonic Test Capability," *Journal of Aircraft*, Vol. 41, No. 3, 2004, pp. 456-463.

[25]Owens, B., Capone, F., Hall, R., Brandon, J., and Chambers, J., "Transonic Free-To-Roll Analysis of Abrupt Wing Stall on Military Aircraft," *Journal of Aircraft*, Vol. 41, No. 3, 2004, pp. 474-484.

[26]Garrell, A., "Development and Demonstration of Calspan's Transonic Free-to-Roll Rig," AIAA-2006-3147, 25th AIAA Aerodynamic Measurement Technology and Ground Testing Conference, June 2006.

[27]Boynton, R.; and Wiener, K.: "High Accuracy Instrument for Measuring Moment of Inertia and Center of Gravity", SAWE PAPER No. 1827 presented at the 47th Annual Conference of the Society of Allied Weight Engineers, 1988.

[28]Snow, W. L.; Childers, B. A.; Jones, S. B.; and Fremaux, C. M.: "Recent Experiences with Implementing a Video Based Six Degree of Freedom Measurement System for Airplane Models in a 20-Foot Diameter Vertical Spin Tunnel", *Proceedings of the SPIE Videometrics Conference*, Volume 1820, 1992, pp. 158 - 180.

[29]Owens, D.: Spin-Tunnel Investigation of a 1/28-Scale Model of the LTV YA-7F Airplane, NASA CR-198225, 1995.

[30]Fremaux, C. M., Vairo, D. M., and Whipple, R. D.: Effect of Geometry and Mass Distribution on the Tumbling Characteristics of Flying Wings, Journal of Aircraft, vol. 32, number 2, 1995, pp. 404 – 410.

[31]Mitcheltree, R. M., and Fremaux, C. M.: Subsonic Dynamics of Stardust Sample Return Capsule, NASA TM-110329, 1997.

[32]Mitcheltree, R. A., Fremaux, C. M.; and Yates, L. A: "Subsonic Static and Dynamic Aerodynamics of Blunt Entry Vehicles", AIAA paper 99-1020, 1999.

[33]Jordan, T.L., Foster, J.V., Bailey, R.M., and Belcastro, C.M., "AirSTAR: A UAV Platform for Flight Dynamics and Control System Testing," AIAA 2006-3307, 25th AIAA Aerodynamic Measurement Technology and Ground Testing Conference, June 2006.

[34]Motter, M.A., "Simulation to Flight Test for a UAV Controls Testbed," AIAA 2006-3305, 25th AIAA Aerodynamic Measurement Technology and Ground Testing Conference, June 2006.

[35]Owens, D.B., Cox, D.E., and Morelli, E.A., "Development of a Low-Cost Sub-Scale Aircraft for Flight Research: The FASER Project," AIAA 2006-3306, 25th AIAA Aerodynamic Measurement Technology and Ground Testing Conference, June 2006.

[36]Levine, J.S., et al., "Science from a Mars Airplane: The Aerial Regional-scale Environmental Survey (ARES) of Mars," AIAA 2003-6576, 2003.

[37]Whipple, R. D.: "Current Perspectives on Emergency Spin-Recovery Systems". Invited Paper, Society of Flight Test Engineers 13th Annual Symposium, New York, New York, September 1982.